Psychedelics Align Brain Activity with Context

Devon Stoliker[1], Leonardo Novelli[1], Moein Khajehnejad[1], Mana Biabani[1], Tamrin Barta[1], Matthew D. Greaves[1], Martin Williams[2], Sidhant Chopra[3,4], Olivier Bazin[5], Otto Simonsson[6], Richard Chambers[7], Frederick Barrett[8], Gustavo Deco[9], Anil Seth[10,11], Katrin H. Preller[12], Robin Carhart-Harris[13,14], Suresh Sundram[15], Gary F. Egan[1,16], Adeel Razi[1,16, 17,18*]

[1]Turner Institute for Brain and Mental Health, School of Psychological Sciences, Monash University, Australia.
[2]School of Health Sciences, Swinburne University of Technology, Hawthorn, VIC 3122, Australia.
[3]Orygen, The University of Melbourne, Parkville, Australia.
[4]Centre for Youth Mental Health, The University of Melbourne, Australia.
[5]British Association of Mindfulness-based Approaches (BAMBA) Listed Teacher, Oxford, UK.
[6]Department of Neurobiology, Care Sciences and Society, Karolinska Institute, Sweden.
[7]Monash Centre for Consciousness and Contemplative Studies, Monash University, Melbourne, Australia.
[8]Department of Psychiatry and Behavioral Sciences, Center for Psychedelic and Consciousness Research, Johns Hopkins University School of Medicine, Baltimore, MD, USA.
[9]Center for Brain and Cognition, Theoretical and Computational Group, Universitat Pompeu Fabra/ICREA, Barcelona, Spain.
[10]Sussex Centre for Consciousness Science, Department of Informatics, University of Sussex, Brighton, UK.
[11]Program on Brain, Mind, and Consciousness, Canadian Institute for Advanced Research, Toronto, Canada.
[12]Department of Adult Psychiatry and Psychotherapy, Psychiatric University Clinic Zurich and University of Zurich, Switzerland.
[13]Centre for Psychedelic Research, Department of Brain Sciences, Imperial College, London, London, UK.
[14]Psychedelics Division, Neuroscape, University of California, San Francisco, USA.
[15]Department of Psychiatry, School of Clinical Sciences, Monash University, Clayton, VIC 3168, Australia.
[16]Monash Biomedical Imaging, Monash University, Australia.
[17]Wellcome Centre for Human Neuroimaging, University College London, United Kingdom.
[18]CIFAR Azrieli Global Scholars Program, Toronto, Canada.

*Corresponding author(s). E-mail(s): adeel.razi@monash.edu;

Abstract

Psychedelics can profoundly alter consciousness by reorganising brain connectivity; however, their effects are context-sensitive. To understand how this reorganisation depends on the context, we collected and comprehensively analysed the largest psychedelic neuroimaging dataset to date. Sixty-two adults were scanned with functional MRI and EEG during rest and naturalistic stimuli (meditation, music, and visual), before and after ingesting 19 mg of psilocybin. Half of the participants ranked the experience among the five most meaningful of their lives. Under psilocybin, functional MRI and EEG signals recorded during eyes-closed conditions became similar to those recorded during an eyes-open condition. This change manifested as an increase in global functional connectivity in associative regions and a decrease in sensory areas. We used machine learning to directly link the subjective effects of psychedelics to neural activity patterns characterised by low-dimensional embeddings. We show that psilocybin reorganised these low-dimensional trajectories into cohesive patterns of brain activity that were structured by context and quality of subjective experience, with stronger self- and boundary-related effects–which were linked to day-after mindset changes—leading to more structured and distinct neural representations. This reorganisation induces a state of 'embeddedness' that arises when brain networks that usually segregate internal and external processing coherently integrate, aligning neural dynamics with context. This state corresponded to profound transformations of perception and self-boundaries, reducing the distinction between self and environment. Embeddedness serves as a bridging framework for understanding both the subjective and therapeutic effects of psychedelics. These findings provide a new account of the large-scale neurocognitive effects of psychedelics and

demonstrate the utility of using machine learning methods in assessing state- and context-dependent neural dynamics and their association with psychological outcomes.

Introduction

The profound effects of psychedelics reshape subjective responses to internal and external sensations and are frequently reported as among the most meaningful experiences in life (Griffiths et al., 2006). These states can manifest sustained therapeutic benefits, including reductions in depression, anxiety, and addiction, alongside increases in social connectedness and overall well-being (Roseman et al., 2018; Ross et al., 2016; Griffiths et al., 2016; Carhart-Harris et al., 2016; Bogenschutz et al., 2015; Pokorny et al., 2017; Kettner et al., 2021; Lyons and Carhart-Harris, 2018). Understanding how contexts influence these changes, and the underlying brain connectivity that can be harnessed clinically, requires a comprehensive examination of how psychedelics reshape the brain's functional integration.

The brain constructs perception and selfhood by integrating external sensory inputs with internal models of the environment (Friston, 2010). These interactions between sensory and associative brain regions are enabled by structural and functional connectivity (Sporns et al., 2005). Psychedelics such as psilocybin disrupt these interactions by acting as an agonist at the serotonin 5-HT_{2A} receptor, inducing structural and functional plasticity that can reshape macro-level connectivity (Ly et al., 2018; Kwan et al., 2022; Burt et al., 2021; Shao et al., 2021; Schmidt et al., 2024). Studies that examine effective connectivity further suggest that associative network communication becomes reconfigured (Stoliker et al., 2023, 2024a,b; Preller et al., 2019; Avram et al., 2024). Reflecting this reorganisation, individuals frequently report an intensified sense of immersion, in which context of space, time, and selfhood feel deconstructed and interconnected (Swanson, 2018)—though the exact mechanisms linking network-level shifts to subjective experience remain unknown. A central mediator of these effects is the default mode network (DMN), which supports the integration of information from diverse associative regions spanning spatial, temporal, and self-referential contexts (Greicius et al., 2003; Raichle et al., 2001; Margulies et al., 2016; Palhano-Fontes et al., 2015; Gattuso et al., 2022; Smallwood et al., 2021). Under psilocybin, constraints on these networks relax, permitting novel patterns of connectivity between sensory and associative regions (Tagliazucchi et al., 2014). This reconfiguration alters crucial connectivity that underlies emotion, cognition, and perception (Preller and Vollenweider, 2018). Notably, preclinical and recent human research suggests that reductions in DMN and anterior hippocampus connectivity may contribute to the therapeutic effects of psilocybin (Siegel et al., 2024; Reinwald et al., 2023).

However, despite mounting evidence for these shifts in connectivity, existing studies often rely on smaller sample sizes or limited experimental contexts (Mediano et al., 2024), making it difficult to generalise how psilocybin alters functional integration across a variety of naturalistic conditions. Furthermore, few investigations combine multiple imaging modalities (Carhart-Harris et al., 2016; Timmermann et al., 2023), behavioural measures and analytical methods to capture both large-scale brain activity and detail fine-grained interactions. We acquired the largest single-site psychedelic neuroimaging dataset to date, integrating multimodal fMRI and EEG with controlled contextual manipulations across eyes-open and eyes-closed states in a predominantly psychedelic-naïve cohort (N=62). Experimental conditions of rest, mindfulness meditation, music, and movie viewing were systematically varied, and extensive behavioural measures were collected (see Fig. 1).

Combining multimodal neuroimaging, diverse contextual manipulations, and multiple analytical methods revealed that the brain shifts towards internally generative (associative) processes over sensory processes under psilocybin. Using state-of-the-art machine learning (ML) techniques we uncovered hidden coherence in brain activity that was structured by context and covaried with the strength of self- and boundary-dissolving effects.

This work underscores the basic and clinical relevance of context-focused research in enhancing and tailoring responses to psychedelics, suggesting a state-dependent neural signature of 'embeddedness' emerges when connectivity and perception become flexibly integrated and aligned with context. We identify this key feature of the psychedelic brain state as psychologically adaptive and contextually modifiable, and introduce new methods for studying mental state and context-dependent neural dynamics in basic and clinical research.

Integration increased in associative areas and decreased in sensory areas

Psilocybin induced distinct shifts in global integration of functional connections across brain regions. This was quantified using Global Functional Connectivity (GFC), a measure of the average correlation of BOLD signals between each vertex and every other vertex in a high-resolution cortical surface map (Cole et al., 2010). During eyes-closed states, psilocybin reduced the GFC of sensory regions (Fig. 2a), and these reductions formed statistically significant clusters (see Fig. Extended Data 1). Occipital areas showed the strongest decrease in GFC (percentage changes up to -39% and Cohen's $d = -0.55$), with midline ventral parietal areas showing strongest decreases during music. In contrast, GFC increased in associative areas (percentage changes up to $+72\%$, Cohens $d = 0.53$). This evidence indicates that, during eyes-closed conditions, psilocybin suppressed the integration of sensory regions with the broader cortical network but enhanced the integration of associative regions. In contrast, eyes-open movie-watching increased GFC in both sensory and associative areas (Fig. 2a), enhancing global synchrony. We confirmed this was not due to head motion Fig. Extended Data 2. Notably, GFC in the temporoparietal junction remained elevated across

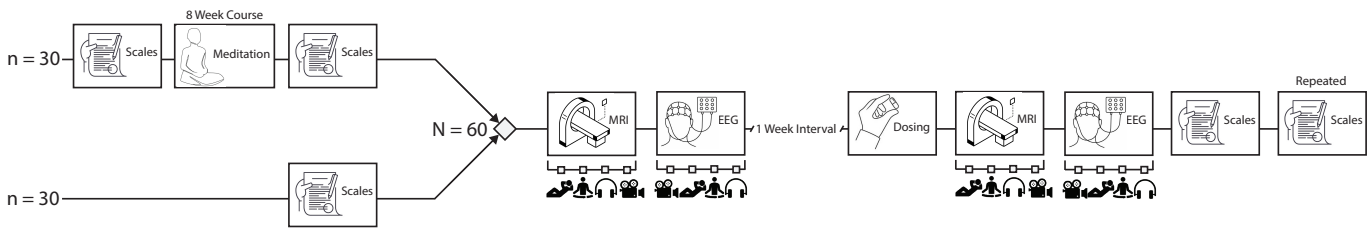

Fig. 1 Simplified representation of study design. Participants were assigned to 8 week mindfulness meditation course or immediately enrolled to multimodal (fMRI and EEG) imaging sessions. An open label 'baseline' (no-psilocybin) imaging session was conducted approximately one week before imaging under administration of 19 mg psilocybin. Music, mindfulness, personality and psychedelic measures were collected before and longitudinally after psilocybin. Meditators received additional assessments before and after the mindfulness course. Meditation showed no differences in our connectivity and subjective effect analyses, and was subsequently collapsed into the main arm for group level analyses. See Methods for details.

both eyes-open and eyes-closed states, suggesting its consistent involvement in the integration of associative processes under psilocybin.

Further analyses using Z-scoring and global signal regression were performed to resolve previous contradictory findings that used smaller samples, where GFC changes differed across datasets and flipped sign after global signal regression (Preller et al., 2018, 2020; Timmermann et al., 2023). Our analyses produced consistent group-level findings for all eyes-closed conditions, confirming the robustness of the observed effects in our large sample (see Fig. Extended Data 3). However, the movie-watching results changed after GSR and z-scoring, demonstrating that applying these transformations can twist the interpretation of GFC. In the Methods, we provide a mathematical explanation for why it happens and recommend not performing GSR and z-scoring in GFC analysis. Despite the consistent group-level findings, substantial variability in GFC changes was observed between participants, indicating individual differences in response to psilocybin (see Fig. Extended Data 4).

Spatially and context-dependent increase of BOLD signal variance

Mapping the standard deviation (SD) of the BOLD signal within subjects across the cortex revealed that signal variability is spatially reorganised and contextually-dependent under psilocybin. Compared to baseline, the SD increased during eyes-open states in the orbitofrontal cortex, occipitotemporal gyri, inferior temporal lobes (particularly anterior regions), and the right hemisphere primary somatosensory cortex. In contrast, SD decreased in early visual areas, in alignment with previous findings on visual imagery (Michaiel et al., 2019). During eyes-open movie watching, we also detected spatially constrained SD increases in early visual regions, as well as the posterior cingulate cortex and precuneus (Fig. 2b), which otherwise showed widespread increases across the brain in other contexts.

SD increases and GFC increases were partially lateralised to the right hemisphere during eyes-closed rest, meditation and music and decreases in sensory regions under psilocybin during eyes-closed conditions, particularly the occipital lobe during music (Fig. 2b). Finally, the spatially dependent redistribution of functional variability across the brain during eyes-open and eyes-closed states was broadly consistent with GFC spatial changes during psilocybin-induced states (Fig. 2a). Increased BOLD signal variability under psychedelics has been commonly associated with increased entropy (Carhart-Harris et al., 2014; Herzog et al., 2023; Viol et al., 2019).

Reduced Separation Between Eyes-Open and Eyes-Closed States

Complementing the spatial maps of GFC changes, we examined the frequency of GFC values across all cortical vertices, independent of their spatial organisation. Under psilocybin, the histograms of GFC values in eyes-open and eyes-closed states—which were distinct at baseline (no-psilocybin) imaging—overlapped (Fig. 2d).

This convergence was consistent and statistically significant across sensory, limbic and associative resting-state networks (RSN) (Fig. 2c and Fig. Extended Data 5) but particularly pronounced in the visual network, where the gap between eyes-closed and eyes-open GFC values decreased by 85% after psilocybin (Cohen's $d = -3.23$, $p < 10^{-307}$). These findings demonstrate that psilocybin-induced spatial changes in GFC synchronise the overall frequency of GFC values between eyes-closed and eyes-open states.

Decreased functional modularity

A significant reduction in functional modularity was observed under psilocybin, suggesting decreased functional segregation. Previous studies with smaller cohorts have reported disruptions in RSN organisation (Tagliazucchi et al., 2016), primarily focusing on default mode network connectivity (Carhart-Harris et al., 2012). Our larger dataset confirms and extends these findings by demonstrating more robust evidence of psychedelic reorganisation of the integration and segregation of brain network architecture. All canonical RSNs (Schaefer et al., 2018; Tian et al., 2020) showed a widespread reduction in functional connectivity; however, the correlation decreased more for brain regions within the same networks than between them (Fig. Extended Data 6), resulting in a net reduction in network modularity (Fig. 2e; Cohen's $d = -0.76, -0.74, -0.85, -0.88$ and Mann-Whitney U-test right-tailed p-values $= 0.000017, 0.000084, 0.000006, 0.000008$, for resting state, meditation, music, and movie conditions, respectively).

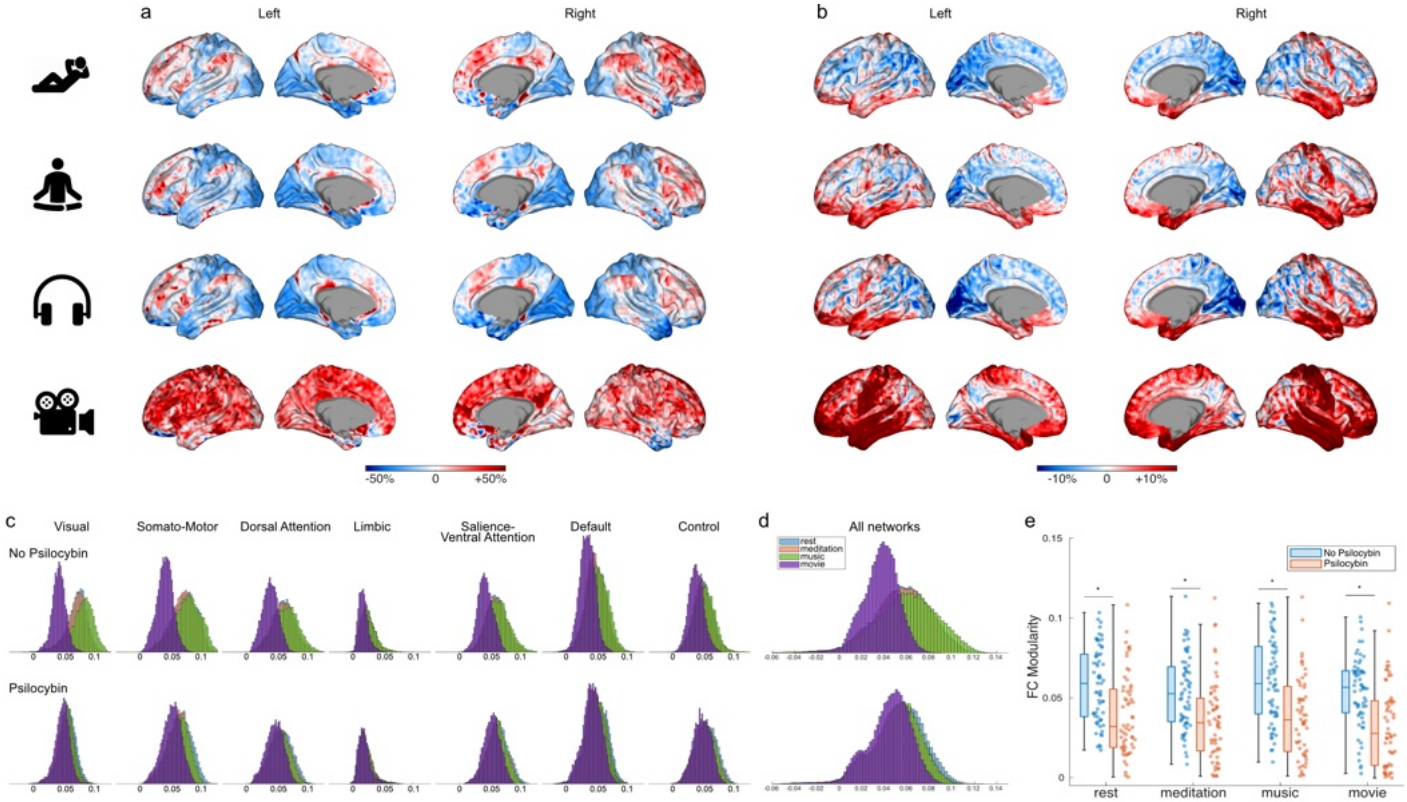

Fig. 2 a) Global functional connectivity (GFC) percentage change (psilocybin vs no-psilocybin) averaged across all subjects for each condition (row). The significant clusters after threshold-free cluster enhancement are shown in Fig. Extended Data 1. b) Standard deviation percentage change (psilocybin minus baseline (no-psilocybin)) computed for each subject and then averaged across subjects, for each condition. c) Histograms of GFC values for 7 resting-state networks (columns) and 4 conditions (colour-coded). The gap between the three eyes-closed conditions vs eyes-open movie-watching at baseline (no-psilocybin) (top row) vastly reduces after psilocybin (bottom row). The baseline gap is most prominent for the visual, sensory-motor, and dorsal-attention networks. d) Histograms of GFC values combining all networks. e) Psilocybin reduces functional connectivity modularity across conditions (Cohen's $d \leq -0.74$). Each point corresponds to one participant, the boxes indicate the quartiles, and the whisker length is 1.5 times the interquartile range. Asterisks indicate a significant decrease based on the Mann-Whitney U-test (all p-values $< 10^{-4}$).

Acute effects classified by neural embeddings

Dimensionality reduction methods have been adopted in neuroscience for uncovering meaningful low-dimensional structures in neural data (Cunningham and Yu, 2014). In ML, the term *embedding* refers to mathematical functions that map high-dimensional data to lower-dimensional representations while preserving essential contextual and semantic information in the lower-dimensional representations. When applied to neural data, it allows to uncover hidden patterns underlying the brain's very high-dimensional complex neural interactions, analogous to manifolds (Pillai and Jirsa, 2017; Fousek et al., 2024; Perl et al., 2025). Here, we used CEBRA to generate low-dimensional embeddings of neural activity and trained a support vector machine (SVM) classifier to test how well session-specific embeddings distinguished between rest, meditation, music, and movie conditions (Schneider et al., 2023) (see Methods for CEBRA description). We then examined the relationship between classification accuracy and subjective experiences assessed via the Mystical Experience Questionnaire (MEQ30)(Barrett et al., 2015), administered at the end of the session

We observed distinct shifts in embeddings associated with subjective ratings of psychedelic effects. Notably, stronger subjective effects were associated with tighter clustering of time point embeddings within the same condition, making them more easily separable from embeddings of other conditions (Fig. 3a). Importantly, this condition-specific clustering was moderated by the timing of subjective effects, as demonstrated by a participant who reported late-onset of substantial effects but minimal subjective experience during the imaging session (Fig. 3b). Their embeddings resembled baseline (no-psilocybin) scans, indicating that the observed neural reorganisation directly reflects the occurrence and intensity of subjective effects within the imaging window (Fig. 3b).

Further analysis of the top five and bottom five MEQ scores reinforced these findings, revealing a gradient in neural embeddings that scaled with strength of subjective effects (Fig. Extended Data 7). This gradient reflects a reorganisation of neural trajectories under psilocybin that is both context-specific and effect-dependent, suggesting that context (rest, meditation, music, or movie) shapes the emergent patterns of neural activity in unison with subjective effects that amplify the cohesion of these patterns.

Next, using the CEBRA-derived trajectories, we classified the condition label for each time point for each participant with a Support Vector Machine (SVM) classifier. We examined the correlation between classification accuracy and each of the 11-Dimension Altered States of Consciousness (11-D ASC) (Studerus et al., 2010) and Mystical Experiences Questionnaire (MEQ30) (Barrett et al., 2015) scores, after psilocybin administration.

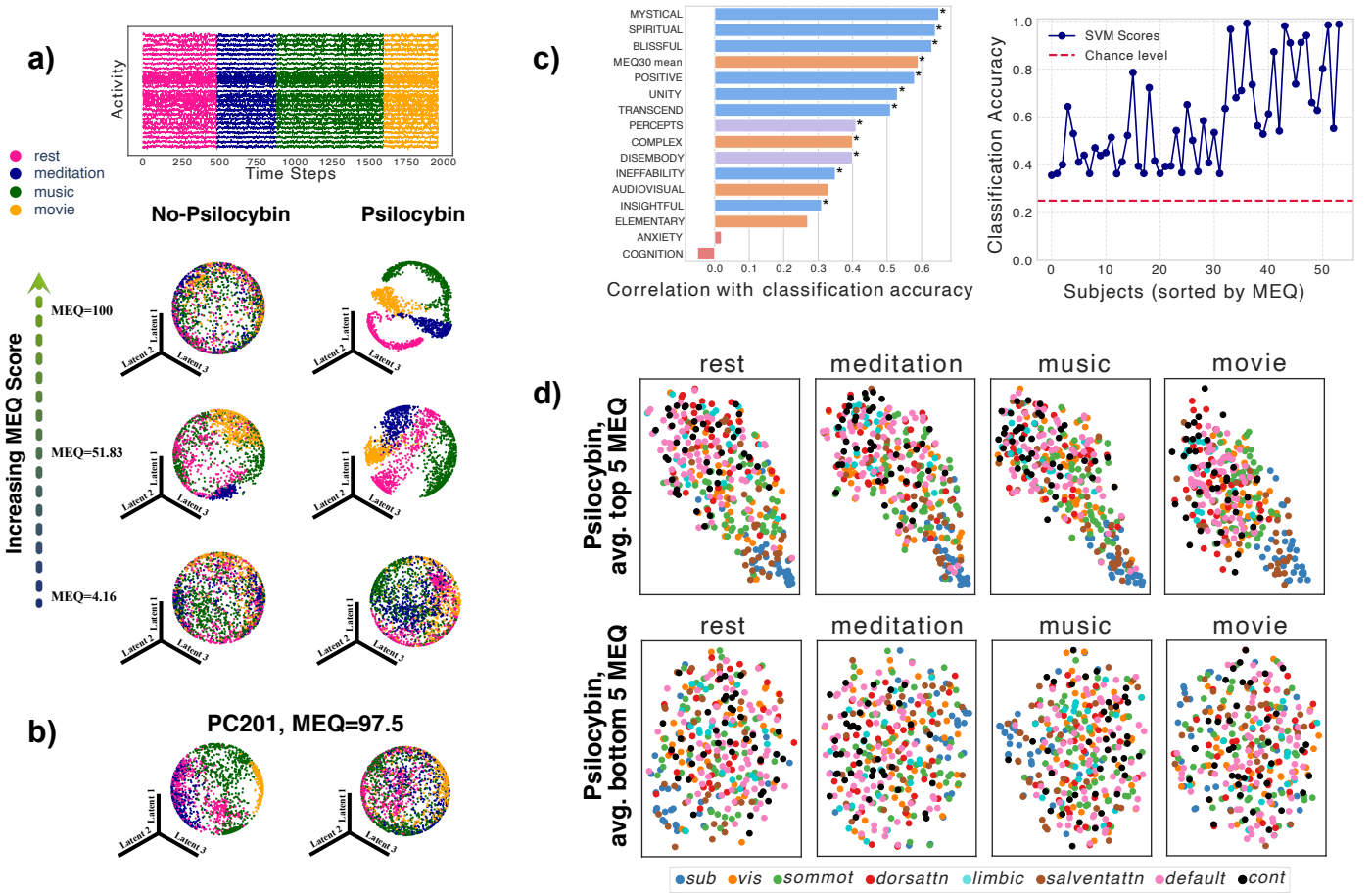

Fig. 3 Psilocybin reorganises BOLD activity along low-dimensional trajectories that scale with subjective effects. a) Using CEBRA—a machine learning method that decodes neural activity over time using contrastive learning—for each participant, we mapped the BOLD time series of all 332 brain parcels at each time point into a 3D space, resulting in a trajectory spanning the entire duration of the four tasks. The pink segment represents rest, while the blue, green, and yellow segments represent the meditation, music, and movie conditions, respectively. b) Network embeddings (CEBRA-derived trajectories) for participant PC201, who reported no subjective effect onset during the MRI session on the day of psilocybin administration, showing similarity to their baseline (no-psilocybin) scan. This suggests that neural embedding changes depend on the alignment of subjective states within the imaging time frame. c) For each participant's CEBRA trajectory, a Support Vector Machine (SVM) was used to classify the correct condition label for each time point. The left panel shows the Pearson correlation between the classification accuracy and acute psilocybin subjective effects including 11 Dimensions of Altered States of Consciousness (11D ASC) and Mystical Experiences Questionnaire (MEQ30) scores. Colours indicate subgroups: Blue = positively felt (euphoric) associative effects; Orange = sensory effects; Red = negatively felt (dysphoric) associative effects; Purple = other (combination) effects. * indicates statistical significance (see Fig. Extended Data 8) . The right panel displays the classification accuracy for each subject, compared to the chance level of 0.25, across the four conditions. Subjects are ordered in ascending order based on their MEQ scores. d) A Temporal Attention-enhanced Variational Graph Recurrent Neural Network (TAVRNN) was used to map the 332 ROIs into a 2D space during each condition. The top row displays the average 2D embedding for participants with the top five highest MEQ scores, while the bottom row shows the average embedding for those with the bottom five lowest MEQ scores. Each node corresponds to one ROI and nodes are colour-coded based on their brain network.

A stronger association was observed between classification accuracy and positively felt associative effects (blue bars), while weaker correlations were found between classification accuracy and sensory effects (orange bars) and low or negative correlation was found for negatively felt associative effects (red bars) (Fig. 3c, left panel and Fig. Extended Data 8). See the next section for conceptual colour-coding and see Methods: Reported measures for details. We also found a correlation between classification accuracy and average mindset changes one day after psilocybin (see Fig. Extended Data 8, Supplementary Material, and the section on subjective effect correspondence with day-after mindset changes). Subjects with higher MEQ30 mean scores generally exhibited higher classification accuracy, indicating a positive relationship between mystical experiences and model performance (Fig. 3c, right panel). These findings suggest embeddings are indicative of the abstract and existential qualities of the experience (i.e., self- and boundary-dissolving effects), as well as positive psychological adjustment which were correlated (see section Subjective effect correspondence with day-after mindset changes), suggesting they may predict the translation of interconnection experienced during the acute psychedelic state to the period after psilocybin.

These results were further supported using another ML-based technique called Temporal Attention-enhanced Variational Graph Recurent Neural Network (TAVRNN) (Khajehnejad et al., 2024), which effectively captured a lower-dimensional representation of individual network connectivity during each of the four conditions. TAVRNN captures temporal changes in network structure by modelling sequential snapshots of neuronal connectivity, enabling the identification of key connectivity patterns and shifts in communicability (see Methods for TAVRNN details). TAVRNN revealed two distinct patterns under psilocybin. Nodes within individual networks exhibited tighter clustering,

reflecting more internally cohesive neural dynamics, reducing within-network separation. See Supplementary Material and Fig. Extended Data 9 for quantification. Simultaneously, embeddings across all networks showed tighter clustering, indicating a shift toward integration of brain-wide organisation and increased global cohesion across contexts. This dual pattern of local within-network cohesion alongside global reorganisation scaled with subjective effects, suggesting that integration depends on subjective experience and is broadly preserved across contexts (Fig. 3d).

Phenomenological structure of psychedelic experience

Participants' reports one day after psilocybin confirmed that their psychedelic experience during imaging were profoundly altered and meaningful. Half of participants retrospectively ranked it among the top five most meaningful experiences of their lives (Fig. 4a), and most reported it as substantially intense (¿9/10) (Fig. 4b). We also collected semi-structured reports one day after psilocybin, with key excerpts describing the experience as "one of the most peaceful and profound things I could ever experience", "...meld[ing] with the MRI machine, floor, walls, air", "los[ing] the plot of who I was, where I was, if I was even here, what was happening" and "los[ing] all sense of self... bec[oming] at one with all my surroundings...as part of a bigger network of things" (see Supplementary Material for a table of qualitative excerpts).

Our large sample enabled a view of within-group subjective reports given a standardised dose of psilocybin. We report histograms and radar plots of 11D ASC and MEQ30 scores that illustrate substantial group-level subjective effect intensity across key scales and wide individual variability from the 19mg dose (Fig. 4c,d,e,f). We colour-coded subscales to reflect a key theoretical and conceptual distinction in psychedelic effects: blue for positively felt associative effects (self- and boundary-dissolving experiences) which are more abstract and existential effects (e.g., transcendence, bliss, unity); orange for sensory effects (e.g., visual imagery, synaesthesia); red for dysphoric effects (e.g., impaired control and cognition, and anxiety); and purple for uncategorised effects. Positively felt associative effects such as bliss and unity received higher ratings across our sample than cognitive insights or spiritual experiences. Negative effects, particularly anxiety, were infrequent or rated as low. These subscales were analysed post hoc to assess patterns of covariation (Vollenweider and Kometer, 2010). This identified subsets of subscales showed high intercorrelations in our sample (Fig. 4g). A complete matrix of 11D ASC and MEQ pairwise correlations is also provided (see Fig. Extended Data 10).

The Life Attitudes Profile Revised (LAP-R) (Reker, 1992) was used to assess death acceptance and changes in personal meaning before and one month after psilocybin administration. Results showed statistically significant group-level improvements in death acceptance (p = 0.0006, d = 0.49) and personal meaning (p = 0.0004, d = 0.51), alongside individual variability (Fig. Extended Data 11). The Nature Relatedness Scale (Nisbet and Zelenski, 2013) was also administered before and one month after psilocybin to assess changes in participants' connection to nature, with results indicating both group-level increases (t(55) = -3.37, p = 0.0014, d = 0.26) and individual shifts (Fig. Extended Data 12)

Our sample's scores were comparable to those observed in higher-dose studies (300-400µg/kg, body-weight adjusted) (e.g., blissful state, experience of unity) (Hirschfeld and Schmidt, 2021), supporting the potential relevance of broader contextual factors we employed, such as space design, minimising interruptions, depth-focus music, and encouraging inward focus, in priming the states examined during imaging.

Subjective effect correspondence with day-after mindset changes

We examined the relationship between each participant's post-psilocybin mindset change score (measured one day after administration, see Supplementary Material) and their subjective experience scores from the 11-D ASC scale and the MEQ30. Mindset change, assessed across dimensions such as connection to self, others, and nature, as well as patience, harmony, and inner peace, correlated moderately with associative dimensions of the psychedelic experience (see Supplementary Material). Insightfulness showed the strongest correlation ($r = 0.65$, $p = 10^{-7}$), followed by mystical, positive, blissful, and spiritual sub-dimensions ($r = 0.4{-}0.6$, $p < 0.00003$). Sensory effects were less correlated ($r = 0.18 - 0.4$, $p < 0.05$ except for Elementary Imagery), while negative experiences showed minimal associations ($r < 0.1$, not statistically significant) (Fig. 4h). These findings indicate the potential primacy of positively felt associative dimensions (self- and boundary-dissolving effects) in driving positive psychological shifts, with cognitive insights and transcendent states—such as unitive, blissful, mystical and spiritual experiences—being more indicative of mindset changes than sensory or challenging negative effects (anxiety, impaired control and cognition). The observed relationship between these states and psychological shifts provides empirical context for ongoing debates about the necessity of the psychedelic experience for clinical efficacy (Yaden and Griffiths, 2020; Olson, 2020).

Context-dependent hippocampal-cortical effective connectivity modulation under psilocybin

Dynamic causal modelling (DCM) (Friston et al., 2003, 2014; Razi and Friston, 2016) revealed context-dependent changes in effective connectivity from baseline (no-psilocybin) to psilocybin administration between the anterior hippocampus (aHip) and nodes of the core Default Mode Network (DMN). While previous preclinical and post-administration studies have highlighted the role of this circuit in psychedelic-induced plasticity (Shao et al., 2021; Vaidya et al., 1997; Siegel et al., 2024), our findings extend these observations by demonstrating acute, context-specific modulation of aHip-DMN connectivity across distinct sensory and cognitive states. These changes reflect cortico-subcortical interactions, linking circuit-level dynamics to

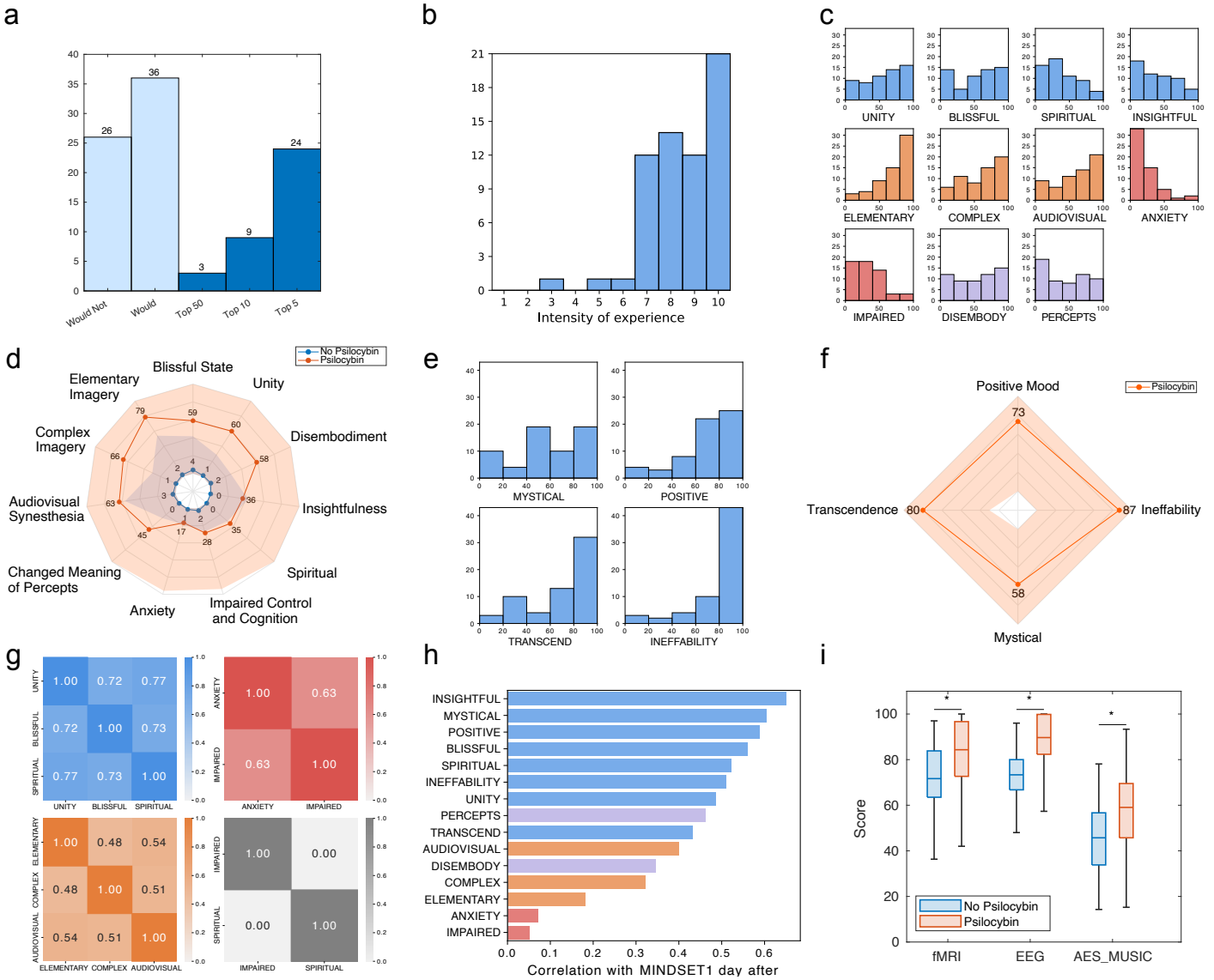

Fig. 4 Phenomenological effects reported by participants. a) Distribution of meaningfulness ratings (see Methods:Reported Measures). The first two bars represent the number of participants who did (second bar) and did not (first bar) rate their experience as personally or spiritually meaningful. The subsequent three bars indicate the number of participants who rated their experience in the top 50, top 10, and top 5 most meaningful life experiences. b) Histogram of intensity scores from the question "How intense would you rate the psilocybin experience?" reported the day after psilocybin, showing most participants rated the effects as substantially intense. c) Histogram of 11 Dimensions of Altered States of Consciousness (11D ASC) scores across participants. Colours indicate general theoretical distinctions: Blue = positively felt (euphoric) associative effects; Orange = sensory effects; Red = negatively felt (dysphoric) associative effects; Purple = other (combination) effects. d) Radar plot of 11D ASC showing minimum-maximum range (shaded) and mean scores (solid line) for dimensions across participants after psilocybin and no psilocybin. e) Histogram of Mystical Experiences Questionnaire scores across participants, composed of four positively felt (euphoric) associative subdimensions and one ambiguous associative subdimension (ineffability). f) Radar plot of MEQ30 showing minimum-maximum range (shaded) and mean scores (solid line) for dimensions across participants. g) Associations between 11D ASC effects reveal strong correlations among positively felt associative effects (blue), sensory effects (orange), and negatively felt associative effects (red). No correlation was found between Impaired Control and Cognition and Spiritual Experience, suggesting their mutual exclusivity across participants. See (Fig. Extended Data 10) for complete matrix of 11D ASC and MEQ within-sample pairwise correlations. h) Correlations between averaged next-day mindset change and acute psilocybin subjective effects (11D ASC and MEQ30), linking each participant's mindset score to their respective subjective effects scores. This approach captures individual variability, highlighting how specific dimensions, like insightfulness or anxiety, relate to subsequent average mindset scores. See Supplementary Material for mindset score dimensions. i) Histogram of Music experience scores, (see methods reported measures) showing ratings of music condition during EEG and MRI with psilocybin and no psilocybin. AES-M are also displayed to change in aesthetic music experience with no psilocybin and psilocybin.

broader transformations in functional connectivity and subjective experience under psilocybin.

Connectivity patterns varied significantly depending on experimental conditions, with left inferior parietal cortex (IPC_L) consistently inhibiting the right anterior hippocampus (aHip_R) across tasks but not at rest. During the resting state, excitation from the posterior cingulate cortex (PCC) to the aHip_R and inhibition from the medial prefrontal cortex (mPFC) to the aHip_R were observed, alongside inhibition from the left anterior hippocampus (aHip_L) to the IPC_L (Fig. 5a, very strong evidence, probability > 99%). These connections suggest a regulatory mechanism, with the PCC driving hippocampal activations, the mPFC attenuating them, and the aHip_L suppressing parietal engagement, potentially amplifying self-reference while limiting evaluation and contextual integration with

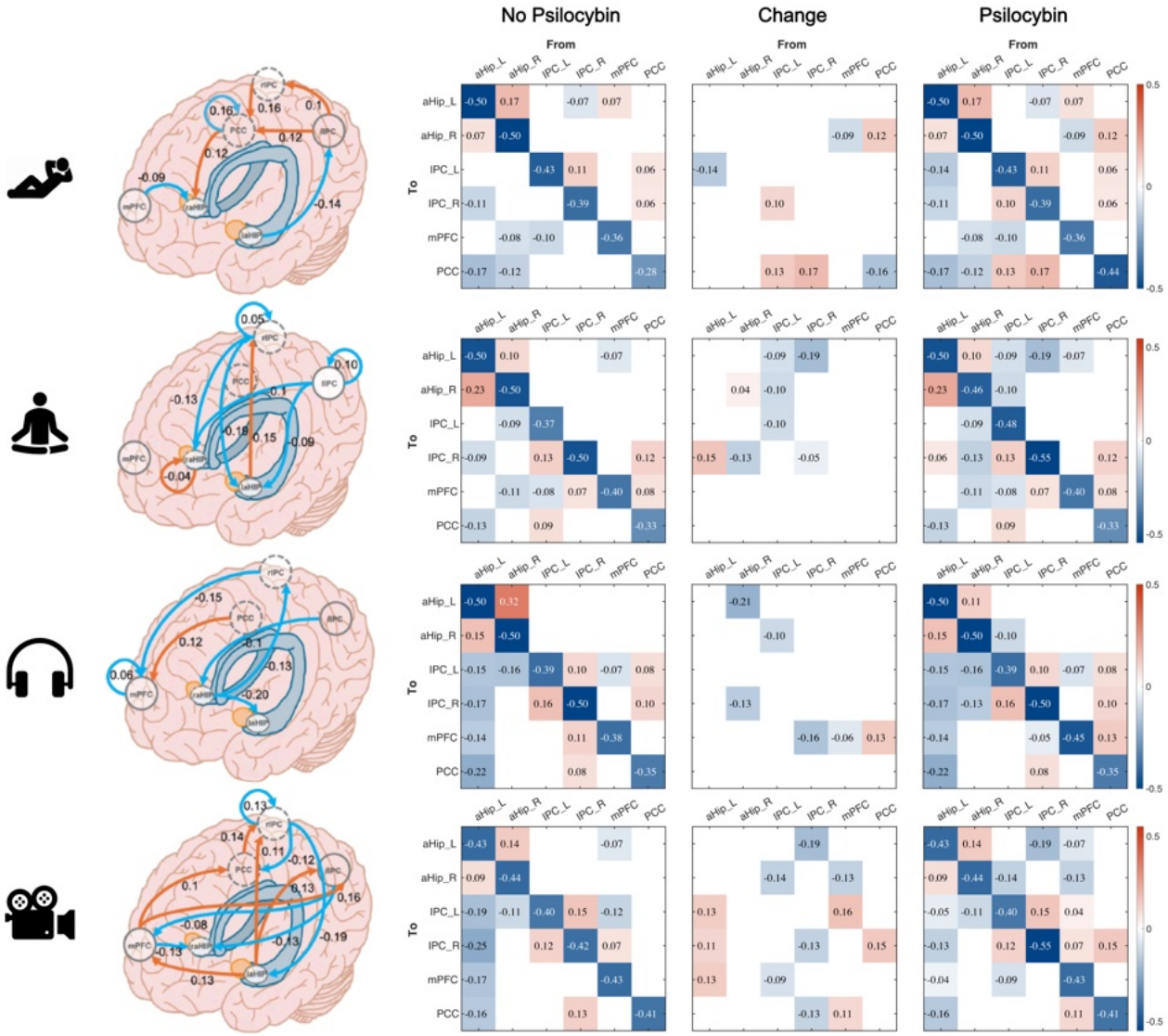

Fig. 5 Model of effective connectivity changes from placebo to psilocybin. Brain regions: Left anterior hippocampus (aHip_L), right anterior hippocampus (aHip_R), left inferior parietal cortex (IPC_L), right inferior parietal cortex (IPC_R), medial prefrontal cortex (mPFC), and posterior cingulate cortex (PCC). Cool colours represent inhibition, while warm colours represent excitation. For self-connections, positive values indicate a shift away from excitation, represented here in cool colours to denote increased inhibition. Rows: Scan sequences – rest, meditation, music, and movie watching. Columns: (1) Spatial mapping of regions of interest and estimated effective connectivity (EC) changes from baseline (no-psilocybin) to psilocybin. (2) Mean EC at baseline for reference. (3) Estimated EC changes from baseline to psilocybin, reinforcing the general trend of mean EC findings and aiding visualisation of psilocybin-induced connectivity changes. These changes are calculated using posterior means of both conditions, averaged at the group level via Bayesian model averaging. (4) Mean EC under psilocybin. Results demonstrate the sensitivity of aHipp-DMN connectivity to context, with context-dependent changes in feedback between the core DMN and anterior hippocampus. Each condition exhibited unique connectivity profiles, with eyes-open movie watching producing complex connectivity changes distinct from the inhibitory patterns typically observed in eyes-closed states. Effect sizes (posterior expectations) of connections are measured in Hz, except for self-connections, which are always inhibitory and log-scaled (see Supplementary Material for details and tables of posterior expectations across conditions and credible intervals for between network connections). Connections displayed have a posterior probability > 0.99, indicating very strong evidence.

memory. During meditation, bilateral inferior parietal cortex (IPC_L and IPC_R) inhibited bilateral anterior hippocampi (aHip_L and aHip_R), consistent with reduced hippocampal-cortical integration associated with focused attentional states and diminished self-referential processing (Fig. 5b). Under music conditions, inhibition from the aHip_R to the aHip_L was observed, potentially altering interhemispheric coordination of memory representations through asymmetric dampening of hippocampal connectivity (Fig. 5c). The strongest connectivity changes were elicited during eyes-open movie stimuli, where inhibition from the IPC_L, IPC_R, and mPFC to the hippocampi and intra-cortical excitation predominated, in response to a shift toward externally driven visual processing. Excitation from the aHip_L to the mPFC, IPC_R, and IPC_L during this condition may indicate heightened integration of narrative memory with evaluative processes, potentially reflecting a redistribution of influence in this network from higher-order regions to subcortical-driven memory integration (Fig. 5d).

The dynamic nature of these connectivity changes highlights how psilocybin supports neural adaptability, providing a temporal window for context-dependent neural reorganisation (Calder and Hasler, 2023). These directed connectivity changes offer mechanistic insights that bridge preclinical and post-psilocybin imaging evidence of hippocampal plasticity in humans with acute mechanisms,

illustrating how set and setting modulate brain function at the circuit level. This suggests that structuring a sensory and cognitive environment can shape neural activity and may be used to guide behavioural outcomes.

Impact of mindfulness meditation training and music on psilocybin effects

Our study included meditation training for half of the participants (Fig. 1). By assigning participants to meditation rather than allowing self-selection, we aimed to assess the clinical utility of structured meditation training before psilocybin while addressing selection bias inherent in meditation-psychedelic studies. Engagement metrics, such as session attendance rates ($\geq$ 6 weeks) and independent practice completion (ave. 85 min per week), indicated consistent participation across the cohort. However, neither differences in acute psilocybin effects nor next-day mindset between meditators and non-meditators (11-D ASC, MEQ30) were statistically significant. Additionally, it did not lead to statistically significant changes in connectivity metrics (Fig. Extended Data 13). Music, a contextual element known to shape subjective experiences under psychedelics (Kaelen et al., 2018), played a central role in the study design. During MRI and EEG sequences, participants listened to ethereal music selected for its potential to enhance emotional depth and transcendence while harmonising with scanner noise. Participants rated the music as significantly more meaningful and emotionally resonant under psilocybin compared to non-psilocybin conditions (15-25% increase with a robust Cohen's d effect size > 0.67 and Mann-Whitney U-test p-values $p < 0.001$). The effect of music used throughout the study design were also verified using the Aesthetic Experiences in Music scale (AES-M) collected at the end of the administration day (Fig. 4i, see Methods: Reported measures for details).

Context-sensitive neural integration under EEG

Context sensitive psychedelic-induced neural dynamics observed using MRI were confirmed using 64-channel wet EEG, both in the power spectrum and in the signal complexity. Our findings extend human and preclincal observations of desynchronised local neural activity under psilocybin in rodent models (Golden and Chadderton, 2022), by revealing that these neural alterations are modulated by sensory context—manifesting robustly in both large-scale MRI and high-density EEG measures. We found that psilocybin expanded the power spectrum, with decreases in theta, alpha, and beta power and increases in gamma during eyes-closed conditions, while movie-watching attenuated these changes, except for gamma increases in early visual areas (Fig. 6a). Meditation and music recordings aligned in EEG, showing similar power profiles across frequencies during no psilocybin and under psilocybin, suggesting a shared introspective neural signature (Fig. 6b). Psilocybin also reduced the difference between eyes-open and eyes-closed alpha power by 48% (robust Cohen's $d = -0.79$, Mann-Whitney U-test right-tailed p-value $< 10^{-19}$), suggesting a unification (or integration) of internally- and externally-focused neural processing (Fig. 6b,c and Fig. Extended Data 14). Signal diversity, quantified via Lempel-Ziv complexity, was highest in eyes-closed conditions (see (Mediano et al., 2024) for similar results), linking internally generated perceptions with enhanced complexity and reinforcing the convergence of meditation and music states (Fig. 6d). Alpha-band activity (8–12 Hz), typically associated with suppressing visual input during eyes-closed conditions (Kometer et al., 2013; Toscani et al., 2010), decreased under psilocybin, particularly in visual regions. This reduced sensory filtering, combined with changes in MRI functional connectivity patterns, suggests diminished distinctions between eyes-open and eyes-closed conditions. The convergence of the MRI and EEG findings confirms that this effect cannot be explained solely by vascular changes caused by psychedelics (Carhart-Harris et al., 2012).

Psilocybin transforms embeddedness in brain and perception

ML embeddings' reorganisation of networks into clusters under psilocybin was linked to positively felt self- and boundary-dissolving subjective effects, (Fig. 3b,d). The relative activation of these networks regulates the balance between internally (e.g., DMN) and externally directed processing, a dynamic that shapes perception and cognition (Fox et al., 2005; Raichle et al., 2001). Their increased integration under psilocybin suggests a shift toward more flexible connectivity and altered functional interactions. The classification accuracy associating degree of integration with self- and boundary-dissolving effects suggests these embeddings capture a connectivity state in which internal and external processes become less distinct. We define this heightened sense of interconnection with the environment as a state of 'embeddedness'. In perceptual terms, embeddedness describes how the self is situated within a broader context. In neurobiological terms, embeddedness describes the functional arrangement of brain regions, showing increased integration within and between networks.

Our construct of embeddedness draws upon computational advances demonstrating that the brain encodes meaningful probabilistic relationships across high-dimensional spaces and adapts flexibly to environmental uncertainty (Ma et al., 2006). We found that CEBRA embeddings formed distinct clusters corresponding to psychological and environmental contexts under psilocybin, but not during imaging with no psilocybin (Fig. 3a,b). Independently, TAVRNN findings suggest that flexible, integrated connectivity aligns with the highly separable domains observed across different contexts in CEBRA (Fig. 3d) These results not only deepen understanding of psychedelic mechanisms but also address a critical gap in systems neuroscience: how large-scale functional (neural) embeddings change under multiple contextual demands in a pharmacologically altered state.

Furthermore, applying ML embedding techniques adds critical nuance to our interpretation of modularity changes. These embeddings revealed that the observed reduction in within-network connectivity, as measured by functional connectivity, is underpinned by coherent within-network

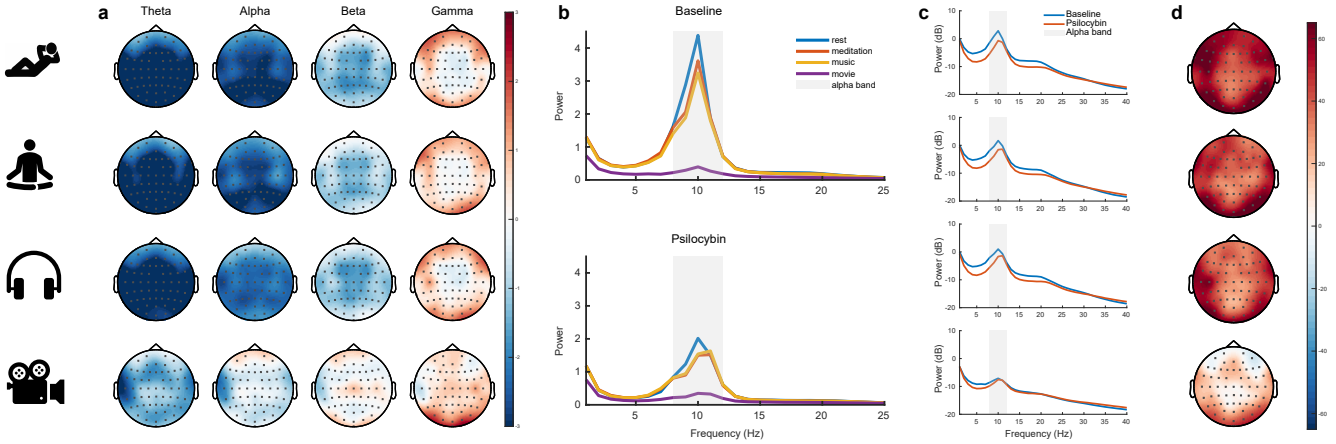

Fig. 6 a) Spatial difference in power (psilocybin minus baseline (no-psilocybin), in dB units) for each frequency. b) Power spectrum (averaged across participants). c) Lempel-Ziv complexity difference (psilocybin minus baseline (no-psilocybin)).

clustering (Fig. 3d). These findings indicates that hidden network integration underlies previous reports of desynchronisation (Siegel et al., 2024).

Moreover, CEBRA embeddings showed that the greatest classification accuracy covaried with positively felt associative subjective effects, which express the emotional and transformative quality of embeddedness (e.g., spiritual, blissful and unitive), while less for sensory and no association with negative effects (Fig. 3c). Additionally, the link we identified between positively felt associative effects and improved mindset (Fig. 4h) was replicated with CEBRA embeddings, showing classification accuracy covaries with improved mindset scores (Fig. Extended Data 8), suggesting these embeddings correspond with psychologically adaptive outcomes. This indicates ML-based embeddings are moderately associated with a brain state where individuals perceive themselves as more integrally connected across personal, social, and ecological spheres.

The interpretation of the positively felt psychedelic state as psychologically adaptive is reinforced by earlier reports of changes to sense of interconnection between self, with others and environment within supportive setting (Watts et al., 2017; Pokorny et al., 2017; Kettner et al., 2021; Lyons and Carhart-Harris, 2018). While future work is needed to test whether ML embeddings generalise across different populations, these methods have significant application for consciousness studies and psychiatry, suggesting embeddings as a novel diagnostic in basic and applied research that are sensitive to pharmacological, psychological and contextual conditions.

Context shaped connectivity

Leveraging a highly powered multimodal dataset and varied set of experimental contexts enabled us to address a major gap in our understanding of context and brain connectivity under psilocybin. Previous research has suggested psychedelics heighten sensory input, thereby increasing the influence of context. We advance this narrative by demonstrating the brain's increased reliance on associative connectivity, moving eyes-closed activity towards a pattern of sensory inputs, as the mechanism which amplifies the influence of context. Using multiple analyses methods, we provided evidence that this increased reliance on associative connectivity transforms how brain activity aligns with psychological and sensory context inputs during the psychedelic state.

The GFC analysis demonstrated the rebalance of sensory and associative connectivity under psilocybin. During eyes-closed conditions, reduced sensory coupling was accompanied by an increased associative coupling, potentially enhancing higher-order processes and amplifying their roles in internally generated perception. These changes suggest psilocybin alters how sensory and associative signals are tuned, with sensory region activity increasing beyond no psilocybin levels when visual input was introduced. Our large-sample size advanced this area of research by clarifying controversial findings from earlier studies investigating whether sensory and associative connectivity would increase, decrease, or flip sign under certain preprocessing steps (Preller et al., 2018, 2020; Timmermann et al., 2023). Further analysis using histograms of GFC values revealed that psilocybin reduced the separation between eyes-open and eyes-closed states, both globally and across individual networks, and was particularly evident in the visual network (Fig. 2c).

Psilocybin also redistributed neural signal variability across sensory and associative networks. Increases in BOLD signal variance of ventral, temporal and somatosensory regions and decreased variance of early visual areas during eyes-closed states aligns with the transition toward associative processing that was observed in our GFC findings. These findings advance lines of evidence relating signal deviation to neural flexibility and entropy (Carhart-Harris et al., 2014; Herzog et al., 2023; Viol et al., 2019), demonstrating how psilocybin reshapes the spatial arrangement of signal dynamics in a context-structured manner.

The 64-channel wet EEG provided a separate modality that confirmed the pattern of context-sensitive changes we identified in fMRI. Reduced alpha-band inhibition we observed during eyes-closed states, under psilocybin, suggests a mechanism for the spontaneous production of internally-generated visual effects (Kometer et al., 2013). Lempel-Ziv complexity increased brain-wide during eyes-closed condition, extending previous evidence of these effects in occipital-parietal regions (Schartner et al., 2017). Music and meditation tuned the power spectrum similarly by reducing alpha power, providing new evidence for a convergent influence of cognitive and environmental context

and their potential synergy. Similar entropy effects of external sitmulation under psychedelics have also been reported (Mediano et al., 2024).

Our analyses also advanced emerging preclinical and human evidence of anterior hippocampus-DMN neuroplasticity following psilocybin (Siegel et al., 2024). For the first time, we demonstrated cognitive and environmental context differentially tune the directed connectivity of these brain circuits beyond their baseline (no-psilocybin) comparison during the acute effects. Our contextual manipulations suggest that curated eyes-open visual stimuli may help clinicians control connectivity changes. This avenue of research, along with the examination of the longitudinal behavioural effects of specific connectivity changes in culturally diverse healthy and clinical populations can advance precision psychiatry and currently remains underexplored.

Critically, our use of ML-based embeddings (CEBRA and TAVRNN) establishes new methods to characterise neural dynamics in neuroimaging research. These neural signatures differentiated patterns of psychedelic brain activity across experimental contexts (e.g., rest, meditation, music, movie), with greater classification accuracy associated with the quality of acute subjective experience, particularly interconnectedness and self-dissolution (e.g., mystical, blissful, unity and related subdimensions). This evidence, based on the increased integration and fluidity of cortical and subcortical network connectivity (TAVRNN) and classification accuracy of ML embeddings (CEBRA), supports the construct of embeddedness, defined as the coherent integration of brain network connectivity that corresponds with positively-felt dissolution of self and interconnection between internal and external experience (i.e., sense of embeddedness), which was linked with subsequent adaptive psychological changes (e.g., mindset transformations, LAP-R scores).

These findings redefine how context modulates perception under psychedelics, shifting the focus from enhanced sensory-driven processing to recognising the overarching role of altered associative processes in psychedelic transformations of perception. ML-derived neural embeddings were key to these advances, highlighting their utility as tools to measure state-dependent effects and forecast personalised behavioural outcomes in precision psychiatry and consciousness research.

Methods

Ethics and clinical trial registration

The study protocol was approved by the Monash University Human Research Ethics Committee. The trial was registered with the Australian New Zealand Clinical Trials Registry under the registration number ACTRN12621001375842.

Study design

The study was open-label and included two imaging sessions: a baseline (no-psilocybin) session and a session following the administration of a 19 mg dose of psilocybin. Both sessions involved MRI and EEG scans, with four conditions repeated in each: resting state, guided meditation, music listening, and movie watching. In the resting-state condition (8 minutes), participants were instructed to relax and keep their eyes closed while remaining still. During the guided meditation (6:30 minutes), participants received brief instructions via MRI-safe audio, followed by silent periods of meditation. For the music listening condition (11:24 minutes), a curated playlist was designed to evoke emotional depth and resonance. In the naturalistic movie condition (6:00 minutes), participants watched a video of moving clouds without audio. These conditions were studied in both the baseline (no-psilocybin) and psilocybin sessions and were repeated in both fMRI and EEG, allowing for comprehensive cross-modal and longitudinal analyses of brain activity and connectivity. The eligible participants were stratified based on age and sex and then randomly assigned to one of the groups. Half of the participants were assigned to an 8-week mindfulness-based cognitive therapy (MBCT) program *Finding Peace in a Frantic World* run by a trained and registered instructor, which involved weekly group meetings and daily independent practice; the other half were assigned to a control group with no intervention. Our decision to administer a standardised dose of 19 mg psilocybin, rather than a body-weight-adjusted dose was based on previous research showing limited benefits of body-weight-adjusted dosing (Garcia-Romeu et al., 2021). The dosage was administered as one oral capsule and selected through consultation multiple collaborators with previous psychedelic imaging experience. This dose was determined to be tolerable for the majority of healthy adults undergoing imaging procedures, while also sufficient to produce significant subjective effects.

Several behavioural measures were collected before and during the baseline (no-psilocybin) and psilocybin scans (see Reported Measures). The follow-up conducted the day after psilocybin administration included semi-structured, open-ended questions and experience ratings. Further follow-up measures were administered one week, and one, three, six and twelve months after psilocybin administration.

Participants

Sixty-five healthy, psychedelic-naive adults aged 18-55 were recruited for the study. Participants were required to have no formal meditation practice and limited previous exposure to meditation. They were first screened via short online survey and then detailed screening was performed by a suitably trained staff member for excluding any psychopathology using the long form SCID-V (First et al., 2015). Exclusion criteria included a history of psychiatric disorders or suicidality, a 5-year history of substance and/or alcohol use disorder, first-degree relatives with a diagnosed psychotic disorder, a history of major neurological disorders including stroke and epilepsy, use of hallucinogens within the last six months, a formal meditation practice in the last 6 months or extensive previous exposure to mindfulness mediation, and contraindicated medications. Participants were also screened for MR contraindications and provided informed consent. On the day of psilocybin administration, they were assisted by a study doctor, researchers, lab staff with relevant training, and volunteers from the community drug harm reduction support

organisation "Dancewize". Individual experiences varied the day after psilocybin administration, with some participants reporting transient headaches during the night (n=3). Three participants required follow-up support from a clinical psychologist familiar with psychedelic integration. These follow-up calls were conducted over the phone, and no further assistance was required. Two participants didn't complete the psilocybin imaging session (neither MRI nor EEG due to psilocybin-induced back pain in one case and an incidental finding on their baseline scan in the other, and one only completed part of the resting-state MRI scan due to adverse responses (a combination of dysphoria, panic, and distressing closed-eye visuals in the MRI), two others didn't complete the second EEG session only due to delayed onset of feeling overwhelmed, and one was excluded because they disclosed having extensive meditation experience at the time of baseline imaging, which was an exclusion criteria. Thus, fMRI raw data is available for sixty-four participants in the baseline session, and sixty-one participants in the psilocybin session. EEG raw data is available for sixty-four participants in the baseline session, and fifty-nine participants in the psilocybin session.

Reported Measures

Reported measures were part of a broader assessment conducted before and longitudinally after psilocybin administration, with a subset integrated into the present analysis. 11-Dimensional Altered States of Consciousness (11D-ASC) scale (66 items) (Dittrich, 1998; Studerus et al., 2010) was administered post-EEG at baseline and at the end of the psilocybin session (approximately 320 minutes after dose) to assess subjective alterations in consciousness. The Mystical Experience Questionnaire (MEQ30) (Barrett et al., 2015) was also collected at this time to measure mystical-type experiences, along with the Aesthetic Experience Scale–Music (AES-M), used to assess the intensity of emotional and aesthetic responses to music. The AES-M scale is derived from the Aesthetic Experience Scale (AES) (Stamatopoulou, 2004), refined through psychometric validation (Silvia and Nusbaum, 2011), and adapted for music-related experiences (Sachs et al., 2016). We adapted the instructions of this measure for collection on the day of psilocybin by asking participants to respond with reference to their musical experience during the psilocybin session. The order of scale presentation was randomised.

One day after psilocybin, participants provided self-reported intensity ratings assessing the perceived strength of the experience, meaningfulness ratings evaluating personal and spiritual significance, and a novel mindset measure capturing changes in psychological state. See Supplementary Material for mindset measure details.

To assess the perceived meaningfulness of the experience, participants were asked: "Would you rate the experience among the most meaningful and spiritually significant experiences of your life?" If they responded yes (n=), they were then asked: "Where would you rate the experience among the most meaningful and spiritually significant experiences of your life?" Response options included top 200 (n=1), top 100 (n=0), top 50 (n=3), top 10 (n=9), and top 5 (n=24).

The Nature Relatedness Scale (NR-6) (Nisbet and Zelenski, 2013) and Life Attitudes Profile–Revised (LAP-R) (Reker, 1992)—assessing death acceptance, coherence, and purpose—were collected before psilocybin and one month post-administration to examine changes in ecological connectedness and existential meaning.

MRI acquisition

Structural MRI data was acquired using a Siemens 3 Tesla Magnetom Skyra scanner at Monash Biomedical Imaging, Monash University, Australia. T1-weighted (T1w) anatomical images were obtained for each participant during two sessions: at baseline (no-psilocybin) and on the psilocybin administration day. The images were acquired using a 3D magnetisation-prepared rapid gradient-echo (MP-RAGE) sequence with a 32-channel head coil. The acquisition parameters were as follows: repetition time (TR) of 2300 ms, echo time (TE) of 2.07 ms, 192 slices per slab, 1 mm slice thickness, and 1 mm isotropic voxel size. The parallel acquisition technique mode used was GRAPPA, with an acceleration factor (PE) of 2 on the baseline day and 3 on the psilocybin administration day. A T2-weighted anatomical image was obtained only during the baseline session. The acquisition parameters were: TR of 3200 ms, TE of 452 ms, 176 slices per slab, 1 mm slice thickness, and 1 mm isotropic voxel size, with an acceleration factor of 2.

Blood-oxygenation-level-dependent (BOLD) fMRI data was collected using a multi-echo, multi-band, echo-planar imaging, T2*-weighted sequence. The acquisition parameters were: TR of 910 ms, multi-echo TE of 12.60 ms, 29.23 ms, 45.86 ms, 62.49 ms, multi-band acceleration factor of 4, field of view of 206 mm, RL phase encoding direction, and 3.2 mm isotropic voxels. The scan durations were: resting state with eyes closed (8 minutes, 505 volumes), audio-guided meditation with eyes closed (6:30 minutes, 405 volumes), music listening with eyes closed (11:24 minutes, 728 volumes), movie watching (6:00 minutes, 372 volumes).

The structural and functional MRI images acquired from the Siemens scanner were converted into the Neuroimaging Informatics Technology Initiative (NIfTI) format and organised according to the Brain Imaging Data Structure (BIDS) 1.7.0.

MRI quality control

Quality control was performed using the MRIQC BIDS app (Esteban et al., 2017), which uses structural and functional MRI images to compute several quality metrics. These include the temporal signal-to-noise ratio and the frame-wise displacement that quantifies head motion (Power et al., 2014). Principal component analysis of these metrics revealed some outliers in the structural and functional images, which were further inspected visually. This process led to the exclusion of 6 structural T1w images from the psilocybin session, while all the T1w images from the baseline session were retained. As for the functional MRI images, 7 subjects had one or more conditions excluded from the analysis, i.e., one or more among rest, meditation, music, or movie. Most of these outliers corresponded

to scans where the head motion was large (mean frame-wise displacement greater than 0.5, which is often used as an exclusion threshold (Parkes et al., 2018)).

MRI preprocessing and cleaning

Anatomical and functional MRI data was preprocessed using *fMRIprep* 22.0.2. The anatomical MRI preprocessing involved correcting T1-weighted images for intensity non-uniformity, skull-stripping, and segmenting brain tissues. The images were then registered, brain surfaces reconstructed, and spatial normalisation performed using the ICBM 152 Nonlinear Asymmetrical template version 2009c (MNI152NLin2009cAsym). The functional MRI preprocessing involved generating a reference volume and skull-stripped version from the shortest echo of each BOLD run, estimating head-motion parameters, and performing slice-time correction. The BOLD reference was co-registered to the T1w reference, confounding time-series were calculated, and the BOLD time-series were resampled into MNI152NLin2009cAsym space.

The preprocessed and optimally combined data produced by *fMRIprep* was cleaned via a single regression in *SPM12* (John Ashburner et al., 2020) using the general linear model. The regressors were: the white matter and cerebrospinal fluid signals computed by *fMRIprep*, the frame-wise displacement, and the non-BOLD components identified via multi-echo ICA performed using *tedana* (version 0.0.12) (DuPre et al., 2021). In short, multi-echo ICA identifies non-BOLD components that are independent of the echo time (Kundu et al., 2012). Finally, to enable surface-based analyses, the cleaned volumetric data was projected to the FreeSurfer left-right-symmetric cortical surface template with 32000 vertices for each hemisphere (fsLR32k).

Standard deviation maps

The standard deviation was computed for the time series of each vertex on the cortical surface. The percentage change (psilocybin vs no-psilocybin) was computed for each participant and then averaged across participants to obtain the mean standard deviation percentage change map shown in Fig. 2b.

Global functional connectivity maps

For each cortical vertex, Pearson's correlation to all other vertices in the same brain hemisphere was computed, transformed to Fisher z-values, and averaged. This calculation yielded a global functional connectivity (GFC) map where each vertex value represents the mean correlation with all other vertices in the same hemisphere (Cole et al., 2010). This generated one map for each participant, in each session (baseline and psilocybin), and each condition (resting-state, meditation, music, movie). The histograms of GFC values were used to compare the sessions and conditions, ignoring the spatial distribution across the cortex (Fig. 2d). To appreciate the spatial distribution, the GFC percentage change was computed (psilocybin day minus baseline, then divided by baseline) for each participant and then averaged across participants, yielding the mean GFC percentage change maps shown in Fig. 2a.

Threshold-free cluster enhancement (TFCE) (Smith and Nichols, 2009) was used to identify significant clusters in the spatial maps without defining arbitrary thresholds for cluster size. Intuitively, TFCE tests all thresholds and gives higher scores to clusters of vertices that are both large and survive increasingly stringent thresholds. TFCE was computed using the PALM software with the default parameters (see https://github.com/andersonwinkler/PALM/blob/master/palm_defaults.m). The statistical TFCE maps were thresholded at $p < 0.05$ with 1000 permutations and a Gamma approximation for the distribution tail (computing permutations is computationally very costly; in our tests, the approximation produced nearly identical clusters to those obtained using 10000 permutations but reduced the computation time by one order of magnitude). Once the clusters of increased and decreased GFC were obtained, they were used to mask the GFC maps of the effect of psilocybin (percentage change) to hide the vertices outside these clusters (Fig. Extended Data 1).

A note on global signal regression and z-scoring the global functional connectivity

We recommend not performing global signal regression (GSR) when computing the GFC, although it has been common practice in previous research (Preller et al., 2020, 2018; Timmermann et al., 2023). Mathematically, GSR alters the covariance matrix of the data such that the average of each row is zero (Murphy et al., 2009). Since GFC is computed by averaging the rows, it would become zero for each vertex across the cortex. The reason why GFC is not exactly zero in the literature using GSR is that the Pearson correlation matrix is used instead of the covariance matrix. The correlation matrix is a rescaled version of the covariance matrix where all the entries are divided by the standard deviations so that they are between -1 and 1. To achieve this normalisation, each entry σ_{ij} of the covariance matrix is divided by the product of the standard deviation of vertices i and j, that is, by $\sqrt{\sigma_{ii}}\sqrt{\sigma_{jj}}$. If all the vertices had the same standard deviation, this normalisation would equally rescale all entries and the average of each row of the correlation matrix would still be zero. In practice, the standard deviation varies across cortical vertices (Fig. 2b) so the average of each row of the correlation matrix is not exactly zero, but typically a small value. We argue that this complicates the interpretation of the GFC, confounding the intended goal of quantifying "the extent to which a cortical vertex is positively/negatively correlated with the other vertices, on average" with "the extent to which a vertex is positively/negatively correlated with vertices having large standard deviation, on average".

Relatedly, plotting z-scored GFC values confounds the interpretation in two ways. If GSR is applied, z-scoring hides the fact that GSR significantly reduces the magnitude of GFC values. More generally, z-scoring is problematic when used to report GFC differences between two conditions. For example, in the main text, we have reported the percentage change between the psilocybin and no psilocybin across conditions (Fig. 2a). Positive and negative values indicate an increase or decrease in GFC, respectively. After z-scoring the changes, this interpretation is no longer possible: a positive z-score only indicates that the change

is higher than average, regardless of its original sign (see Fig. Extended Data 3). If the average were negative, negative values slightly above the average would have a positive z-score.

Parcel-wise FC

The denoised, volumetric data was divided into parcels for further functional connectivity analysis. The Schaefer parcellation (Schaefer et al., 2018) was used to partition the cortical voxels into 300 parcels, each belonging to one of the following 7 resting-state networks: Visual, Somatomotor, Dorsal Attention, Limbic, Salience/Ventral Attention, Default Mode, Control. The Melbourne subcortical atlas (Tian et al., 2020) was used to divide the subcortical voxels into 32 parcels including subdivisions of the striatum, thalamus, hippocampus, amygdala and globus pallidus. (This atlas is specified in voxel space, hence the use of volumetric rather than surface data for this analysis.) Combining the cortical and subcortical parcellations gave a total of 332 parcels. To extract a representative time series for each parcel, the first principal component of the voxel time series within each parcel was computed.

The parcel-wise functional connectivity matrix was obtained by computing Pearson's correlation between the time series of each pair of parcels. The within-network FC was computed by averaging the FC values within the diagonal blocks of the FC matrix, each corresponding to the pairwise correlations between parcels belonging to the same functional network. Similarly, the between-network FC was computed by averaging the FC matrix entries outside the diagonal blocks, i.e., the correlation values between pairs of parcels belonging to different networks (Fig. Extended Data 6). The Mann-Whitney U-test was performed in MATLAB using the 'ranksum' function and the right-tailed option. That is, the alternative hypothesis is that the median within- or between-network FC under psilocybin is lower than the baseline median.

Modularity

The FC modularity was computed using the Brain Connectivity Toolbox (Rubinov and Sporns, 2010) with the 'negative_asym' option for asymmetric treatment of negative weights (Rubinov and Sporns, 2011). The Mann-Whitney U-test was performed in MATLAB using the 'ranksum' function and the right-tailed option. That is, the alternative hypothesis is that the median modularity under psilocybin is lower than the baseline (no-psilocybin) median (Fig. 2e).

Spectral dynamic causal modelling

Spectral dynamic causal modelling (DCM) is a method used to infer the effective connectivity between brain regions from fMRI time series (Friston et al., 2014; Razi et al., 2015; Novelli et al., 2024). Effective connectivity is defined as the influence one neural system exerts over another (Friston et al., 2003), as opposed to functional connectivity, which describes statistical dependencies among BOLD signals (Friston, 2011; Razi and Friston, 2016). DCM employs a forward generative model with neuronal and observation equations. The neuronal model is a linear stochastic differential equation that describes the dynamics of hidden neuronal states. It models how the activity in one brain region is influenced by the activity in other regions, as well as by endogenous fluctuations in neuronal activity. The observation function maps the neuronal activity to the observed BOLD signal by modelling the biophysical processes involved in the haemodynamic response. Spectral DCM estimates the parameters of this model by fitting the generative model to the cross-spectral density of the observed BOLD signals, a second-order statistic that captures the correlations between time series at all time lags (Novelli et al., 2024). By fitting the model to the cross-spectral density, spectral DCM can estimate the effective connectivity between brain regions, as well as the hemodynamic parameters and the spectrum of the endogenous fluctuations. Because DCM is a Bayesian approach, all model parameters are equipped with prior distributions, which are updated based on the observed data to produce posterior distributions over the parameters. Spectral DCM explicitly models the endogenous fluctuations in neuronal activity, which makes it ideal for applications to the resting state and conditions that do not involve strong experimental inputs or block task designs.

Here, we have applied spectral DCM to infer the effective connectivity of each subject in each condition. The analysis focussed on six regions belonging to the DMN, each modelled as a 6 mm sphere centred on the following coordinates: Left anterior hippocampus (aHip_L; X=-26, Y=-16, Z=-20), right anterior hippocampus (aHip_R; X=28, Y=-16, Z=-20), left inferior parietal cortex (IPC_L; X=-44, Y=-60, Z=24), right inferior parietal cortex (IPC_R; X=54, Y=-62, Z=28), medial prefrontal cortex (mPFC; X=2, Y=56, Z=-4), and posterior cingulate cortex (PCC; X=2, Y=-58, Z=30). The subject-level estimates were combined at the group level in a Bayesian fashion, accounting for the varying degree of uncertainty in the estimates across subjects. Specifically, Parametric Empirical Bayes (Zeidman et al., 2019) was used to compute the group-level effective connectivity at baseline and its change under psilocybin (Fig. 5). All DCM analyses were performed using SPM12 (John Ashburner et al., 2020).

CEBRA

Contrastive Embeddings for Behavioural and Neural Analysis (CEBRA) is a self-supervised learning framework that extracts interpretable and consistent low-dimensional embeddings from high-dimensional neural and behavioural datasets (Schneider et al., 2023). By leveraging contrastive learning and auxiliary variables, such as time or behavioural labels, CEBRA enables analyses of population-level trajectories.

In this study, we used CEBRA-Time, a variant of CEBRA tailored for temporal analyses, to explore neural trajectories derived from fMRI data. CEBRA-Time is a contrastive learning-based method designed to extract meaningful latent representations from time series data, such as fMRI signals. It learns a low-dimensional embedding by maximizing temporal coherence while preserving task-related variability, allowing the transformation of high-dimensional neural data into structured latent trajectories.

This enables the discovery of subject-specific neural dynamics in a more interpretable space.

Here, for each participant, we concatenated fMRI time series spanning four consecutive conditions: resting state, meditation, music listening, and movie watching (Fig. 3a). This comprehensive input captured temporal transitions in neural activity across conditions. Applying CEBRA-Time transformed each time point of these high-dimensional fMRI time series into a three-dimensional point in latent space, revealing neural trajectories unique to each subject (Fig. 3a,b). These trajectories provided insights into how dynamic brain activity evolves over different conditions, aligning with self-reported subjective experiences.

TAVRNN

While CEBRA captures overall neural trajectories, a deeper understanding requires analyzing how individual brain regions (ROIs) evolve over time and interact with each other. TAVRNN allows us to track these ROI-specific dynamics and their changing relationships, revealing finer details. This perspective inspired our application of Temporal Attention-enhanced Variational Graph Recurrent Neural Network (TAVRNN)(Khajehnejad et al., 2024). TAVRNN is a framework designed for analysing the temporal dynamics of evolving connectivity networks. TAVRNN is a deep learning framework that models temporal connectivity networks between units of a system by leveraging both structural relationships and past dynamics. Through temporal attention, recurrent neural networks, and variational graph techniques, it learns a lower-dimensional latent representation for each unit (ROIs in this work), preserving meaningful temporal patterns while enhancing interpretability. This allows for tracking the evolution of ROI activities over time, revealing insights into their dynamic interactions. TAVRNN captures both local temporal patterns (how individual ROIs change over time) and global temporal patterns (how the relationships as a whole evolve dynamically). By leveraging latent information from the structure of time-varying functional connectivity networks, TAVRNN enables a robust representation of individual ROI activity and their changing relationships in a low-dimensional space (Fig. 3d). Specifically, a temporal attention mechanism assesses the topological similarity of the network across time steps, incorporating varying time lags to capture complex network dynamics more effectively. This approach is particularly effective in uncovering temporal changes in network structures and their alignment with external behaviours or stimuli.

In our study, we used TAVRNN to analyse functional connectivity (FC) matrices derived from fMRI time series under four consecutive conditions: rest, meditation, music and movie. For each condition, we computed the FC matrices between 332 brain parcels, which served as input nodes to TAVRNN. In this work, each scan under a specific condition (rest, meditation, music, or movie) is treated as a temporal snapshot. Therefore, the attention mechanism enables the lower-dimensional representation of one scan to inform the representation of the subsequent scans. The model then generated two-dimensional embeddings for each parcel, representing their temporal evolution across conditions (Fig. 3d).

EEG acquisition

EEG data was recorded using a 64-channel BrainAmp MR Plus amplifier (Brain Products GmbH, Germany) with BrainVision Recorder software (version 1.22.0001, Brain Products GmbH, Germany) and Ag/AgCl electrodes embedded in an actiCAP slim cap according to the standardized 10-10 system (Chatrian et al., 1985). The FCz electrode served as the reference and the FPz electrode served as the ground for online recording. The impedances were maintained below $10k\Omega$ using an abrasive paste (Nuprep, Weaver and Company, USA) followed by applying a conductive gel (Easycap GmbH, Germany). EEG signals were sampled at 500 Hz with a bandpass filter of $0.01 - 1000Hz$. Participants were comfortably seated in an acoustically absorbent room to minimise environmental noise and their chin strap was securely fastened to ensure head stability. They were instructed to remain as still as possible, avoid jaw clenching, and keep their eyes closed during the recording to minimise artifacts.

The EEG recording session included the same four conditions as the fMRI described above. The naturalistic movie (5 minutes) was presented first, followed by the three eyes-closed conditions: resting state (5 minutes), audio-guided meditation (5 minutes), and music listening (7 minutes). The raw data was acquired as a single continuous recording over all conditions and then split into four separate files using the event markers for the start and end of each condition. Due to technical issues, event markers were not recorded for two participants in the baseline session and one participant in the psilocybin session, so these recordings were excluded from pre-processing and analysis. In summary, pre-processed EEG is available for 63 participants in the baseline session and 58 in the psilocybin session. The EEG data was organised according to BIDS 1.7.0.

EEG pre-processing

The raw EEG signals were preprocessed using the default parameters of the automated RELAX pipeline (Bailey et al., 2023) implemented in MATLAB using functions from EEGLAB (Delorme et al., 2004) and FieldTrip (Oostenveld et al., 2011a) toolboxes. First, the data was bandpass filtered between 0.25 and 80 Hz using a fourth-order Butterworth filter with zero phase, with a notch filter applied between 47 and 53 Hz to reduce line noise. Subsequently, bad channels were removed by applying a multistep process incorporating the "findNoisyChannels" function of the PREP pipeline (Bigdely-Shamlo et al., 2015). This was followed by the initial reduction of the artefacts related to eye movements, muscle activity and drift using a multichannel Wiener filter (Somers et al., 2018), after which the data were re-referenced to the robust average reference (Bigdely-Shamlo et al., 2015). Residual artefacts were then removed by Wavelet-enhanced Independent Component Analysis (WICA) with the artefactual components identified by the automated ICLabel classifier (Hill et al., 2022). Electrodes rejected during the cleaning process were then restored to the data through spherical interpolation. Finally, all pre-processed data were visually inspected for data quality.

EEG data analysis

The power spectrum was computed for all electrodes across all participants using the multitaper frequency transformation ($1-45$ Hz) with a 2-second Hanning window and 50% overlap, implemented in FieldTrip (Oostenveld et al., 2011b). To quantify the effect of psilocybin, the power difference (psilocybin minus baseline) was computed for each channel and then averaged across subjects. The results are reported in Fig. 6 for each condition and four power bands: theta ($4-7$ Hz), alpha ($8-12$ Hz), beta ($13-30$ Hz), and gamma ($30-80$ Hz).

The Lempel-Ziv (LZ) complexity was calculated in two steps using the LZ 1976 algorithm (Lempel and Ziv, 1976). First, the time series for each channel was binarised by setting values above the mean to 1 and values below the mean to 0. The resulting binary sequence was then scanned sequentially to identify distinct patterns and build a dictionary of these patterns. The LZ complexity is given by the number of patterns in the constructed dictionary. Regular signals can be represented by a small number of patterns, resulting in low LZ complexity, while irregular signals have a greater diversity of patterns, leading to higher LZ complexity.

Supplementary Material

See attached file.

Acknowledgements

This research is funded by the Australian Research Council (Refs: DE170100128 and DP200100757) and the Australian National Health and Medical Research Council (Investigator Grant 1194910). A.R. is affiliated with The Wellcome Centre for Human Neuroimaging, supported by core funding from Wellcome [203147/Z/16/Z]. A.R. is a CIFAR Azrieli Global Scholar in the Brain, Mind & Consciousness Program. A.K.S is supported by European Research Council Advanced Investigator Grant CONSCIOUS (Ref: 101019254). K.H.P. is currently an employee of Boehringer Ingelheim GmbH & Co KG.

Data availability

All data reported will be made fully open access through a OpenNeuro repository upon publication.

Code availability

Open-source code for all data analysis pipelines will be made available on GitHub upon publication (https://github.com/razilab). These pipelines used the following software packages: fMRIprep 22.0.2 (https://fmriprep.org), tedana 0.0.12 (https://tedana.readthedocs.io), MRIqc 22.0.6 (https://mriqc.readthedocs.io), MATLAB R2022a (https://www.mathworks.com), SPM12 (https://www.fil.ion.ucl.ac.uk/spm/software/spm12), Freesurfer 7.2 (https://surfer.nmr.mgh.harvard.edu), FSL v.6.0.7 (https://fsl.fmrib.ox.ac.uk/fsl/fslwiki), FieldTrip 20240916 (https://www.fieldtriptoolbox.org). LZ complexity was computed by adapting open-source code by Fernando Rosas and Pedro Mediano (https://information-dynamics.github.io/complexity/information/2019/06/26/lempel-ziv.html). Projection of volumetric fMRI data to the cortical surface was performed by adapting open-source code by Pang et al. available on GitHub (https://github.com/NSBLab/BrainEigenmodes).

References

Avram, M., Müller, F., Preller, K.H., Razi, A., Rogg, H., Korda, A., Holze, F., Vizeli, P., Ley, L., Liechti, M.E., Borgwardt, S.: Effective Connectivity of Thalamocortical Interactions Following d-Amphetamine, LSD, and MDMA Administration. Biological Psychiatry: Cognitive Neuroscience and Neuroimaging **9**(5), 522–532 (2024) https://doi.org/10.1016/j.bpsc.2023.07.010

Bailey, N.W., Biabani, M., Hill, A.T., Miljevic, A., Rogasch, N.C., McQueen, B., Murphy, O.W., Fitzgerald, P.B.: Introducing RELAX: An automated pre-processing pipeline for cleaning EEG data - Part 1: Algorithm and application to oscillations. Clinical Neurophysiology **149**, 178–201 (2023) https://doi.org/10.1016/j.clinph.2023.01.017

Bogenschutz, M.P., Forcehimes, A.A., Pommy, J.A., Wilcox, C.E., Barbosa, P.C., Strassman, R.J.: Psilocybin-assisted treatment for alcohol dependence: A proof-of-concept study. J Psychopharmacol **29**(3), 289–99 (2015) https://doi.org/10.1177/0269881114565144

Barrett, F.S., Johnson, M.W., Griffiths, R.R.: Validation of the revised Mystical Experience Questionnaire in experimental sessions with psilocybin. Journal of Psychopharmacology **29**(11), 1182–1190 (2015) https://doi.org/10.1177/0269881115609019

Bigdely-Shamlo, N., Mullen, T., Kothe, C., Su, K.-M., Robbins, K.A.: The PREP pipeline: Standardized preprocessing for large-scale EEG analysis. Front. Neuroinform. **9** (2015) https://doi.org/10.3389/fninf.2015.00016

Burt, J.B., Preller, K.H., Demirtas, M., Ji, J.L., Krystal, J.H., Vollenweider, F.X., Anticevic, A., Murray, J.D.: Transcriptomics-informed large-scale cortical model captures topography of pharmacological neuroimaging effects of LSD. eLife **10**, 69320 (2021) https://doi.org/10.7554/eLife.69320

Carhart-Harris, R.L., Bolstridge, M., Rucker, J., Day, C.M.J., Erritzoe, D., Kaelen, M., Bloomfield, M., Rickard, J.A., Forbes, B., Feilding, A., Taylor, D., Pilling, S., Curran, V.H., Nutt, D.J.: Psilocybin with psychological support for treatment-resistant depression: An open-label feasibility study. Lancet Psychiatry **3**(7), 619–627 (2016) https://doi.org/10.1016/s2215-0366(16)30065-7

Carhart-Harris, R.L., Erritzoe, D., Williams, T., Stone, J.M., Reed, L.J., Colasanti, A., Tyacke, R.J., Leech, R.,

Malizia, A.L., Murphy, K., Hobden, P., Evans, J., Feilding, A., Wise, R.G., Nutt, D.J.: Neural correlates of the psychedelic state as determined by fMRI studies with psilocybin. Proceedings of the National Academy of Sciences **109**(6), 2138–2143 (2012) https://doi.org/10.1073/pnas.1119598109

Calder, A.E., Hasler, G.: Towards an understanding of psychedelic-induced neuroplasticity. Neuropsychopharmacol. **48**(1), 104–112 (2023) https://doi.org/10.1038/s41386-022-01389-z

Carhart-Harris, R.L., Leech, R., Hellyer, P.J., Shanahan, M., Feilding, A., Tagliazucchi, E., Chialvo, D.R., Nutt, D.: The entropic brain: A theory of conscious states informed by neuroimaging research with psychedelic drugs. Front. Hum. Neurosci. **8** (2014) https://doi.org/10.3389/fnhum.2014.00020

Chatrian, G.E., Lettich, E., Nelson, P.L.: Ten Percent Electrode System for Topographic Studies of Spontaneous and Evoked EEG Activities. American Journal of EEG Technology **25**(2), 83–92 (1985) https://doi.org/10.1080/00029238.1985.11080163

Carhart-Harris, R.L., Muthukumaraswamy, S., Roseman, L., Kaelen, M., Droog, W., Murphy, K., Tagliazucchi, E., Schenberg, E.E., Nest, T., Orban, C., Leech, R., Williams, L.T., Williams, T.M., Bolstridge, M., Sessa, B., McGonigle, J., Sereno, M.I., Nichols, D., Hellyer, P.J., Hobden, P., Evans, J., Singh, K.D., Wise, R.G., Curran, H.V., Feilding, A., Nutt, D.J.: Neural correlates of the LSD experience revealed by multimodal neuroimaging. Proceedings of the National Academy of Sciences of the United States of America **113**(17), 4853–4858 (2016)

Cole, M.W., Pathak, S., Schneider, W.: Identifying the brain's most globally connected regions. NeuroImage **49**(4), 3132–3148 (2010) https://doi.org/10.1016/j.neuroimage.2009.11.001

Cunningham, J.P., Yu, B.M.: Dimensionality reduction for large-scale neural recordings. Nat Neurosci **17**(11), 1500–9 (2014) https://doi.org/10.1038/nn.3776

Dittrich, A.: The standardized psychometric assessment of altered states of consciousness (ASCs) in humans. Pharmacopsychiatry **31 Suppl 2**, 80–4 (1998) https://doi.org/10.1055/s-2007-979351

Delorme, A., Makeig, S., Singh, V., Logothetis, N.K., Panzeri, S., DiCarlo, JJ., Wise, KD., Buzsaki, G., Grivich, M., Sher, A.: EEGLAB: An open source toolbox for analysis of single-trial EEG dynamics including independent component analysis. Journal of Neuroscience Methods **134**(1), 9–21 (2004) https://doi.org/10.1016/j.jneumeth.2003.10.009

DuPre, E., Salo, T., Ahmed, Z., Bandettini, P.A., Bottenhorn, K.L., Caballero-Gaudes, C., Dowdle, L.T., Gonzalez-Castillo, J., Heunis, S., Kundu, P., Laird, A.R., Markello, R., Markiewicz, C.J., Moia, S., Staden, I., Teves, J.B., Uruñuela, E., Vaziri-Pashkam, M., Whitaker, K., Handwerker, D.A.: TE-dependent analysis of multi-echo fMRI with tedana. Journal of Open Source Software **6**(66), 3669 (2021) https://doi.org/10.21105/joss.03669

Esteban, O., Birman, D., Schaer, M., Koyejo, O.O., Poldrack, R.A., Gorgolewski, K.J.: MRIQC: Advancing the automatic prediction of image quality in MRI from unseen sites. PLOS ONE **12**(9), 0184661 (2017) https://doi.org/10.1371/journal.pone.0184661

Friston, K.J., Harrison, L., Penny, W.: Dynamic causal modelling. NeuroImage **19**(4), 1273–1302 (2003) https://doi.org/10.1016/S1053-8119(03)00202-7

Friston, K.J., Kahan, J., Biswal, B., Razi, A.: A DCM for resting state fMRI. NeuroImage **94**, 396–407 (2014) https://doi.org/10.1016/j.neuroimage.2013.12.009

Fousek, J., Rabuffo, G., Gudibanda, K., Sheheitli, H., Petkoski, S., Jirsa, V.: Symmetry breaking organizes the brain's resting state manifold. Sci Rep **14**(1), 31970 (2024) https://doi.org/10.1038/s41598-024-83542-w

Friston, K.: The free-energy principle: A unified brain theory? Nature Reviews Neuroscience **11**, 127 (2010) https://doi.org/10.1038/nrn2787

Friston, K.J.: Functional and effective connectivity: A review. Brain Connectivity **1**(1), 13–36 (2011) https://doi.org/10.1089/brain.2011.0008

Fox, M.D., Snyder, A.Z., Vincent, J.L., Corbetta, M., Van Essen, D.C., Raichle, M.E.: The human brain is intrinsically organized into dynamic, anticorrelated functional networks. Proceedings of the National Academy of Sciences of the United States of America **102**(27), 9673 (2005) https://doi.org/10.1073/pnas.0504136102

First, M.B., Williams, J.B.W., Karg, R.S., Spitzer, R.L.: The Structured Clinical Interview for DSM5 Disorders, Research Version (2015)

Garcia-Romeu, A., Barrett, F.S., Carbonaro, T.M., Johnson, M.W., Griffiths, R.R.: Optimal dosing for psilocybin pharmacotherapy: Considering weight-adjusted and fixed dosing approaches. Journal of Psychopharmacology **35**(4), 353–361 (2021) https://doi.org/10.1177/0269881121991822

Golden, C.T., Chadderton, P.: Psilocybin reduces low frequency oscillatory power and neuronal phase-locking in the anterior cingulate cortex of awake rodents. Scientific Reports **12**(1), 12702 (2022) https://doi.org/10.1038/s41598-022-16325-w

Griffiths, R.R., Johnson, M.W., Carducci, M.A., Umbricht, A., Richards, W.A., Richards, B.D., Cosimano, M.P., Klinedinst, M.A.: Psilocybin produces substantial and sustained decreases in depression and anxiety in patients with life-threatening cancer: A randomized double-blind trial. Journal of Psychopharmacology **30**(12), 1181–1197 (2016) https://doi.org/10.1177/0269881116675513

Greicius, M.D., Krasnow, B., Reiss, A.L., Menon, V.: Functional connectivity in the resting brain: A network analysis of the default mode hypothesis. Proceedings of the National Academy of Sciences **100**(1), 253 (2003) https://doi.org/10.1073/pnas.0135058100

Gattuso, J.J., Perkins, D., Ruffell, S., Lawrence, A.J., Hoyer, D., Jacobson, L.H., Timmermann, C., Castle, D., Rossell, S.L., Downey, L.A., Pagni, B.A., Galvão-Coelho, N.L., Nutt, D., Sarris, J.: Default Mode Network Modulation by Psychedelics: A Systematic Review. Int J Neuropsychopharmacol **26**(3), 155–188 (2022) https://doi.org/10.1093/ijnp/pyac074

Griffiths, R.R., Richards, W.A., McCann, U., Jesse, R.: Psilocybin can occasion mystical-type experiences having substantial and sustained personal meaning and spiritual significance. Psychopharmacology **187**(3), 268–283 (2006) https://doi.org/10.1007/s00213-006-0457-5

Hill, A.T., Clark, G.M., Bigelow, F.J., Lum, J.A.G., Enticott, P.G.: Periodic and aperiodic neural activity displays age-dependent changes across early-to-middle childhood. Developmental Cognitive Neuroscience **54**, 101076 (2022) https://doi.org/10.1016/j.dcn.2022.101076

Herzog, R., Mediano, P.A.M., Rosas, F.E., Lodder, P., Carhart-Harris, R., Perl, Y.S., Tagliazucchi, E., Cofre, R.: A whole-brain model of the neural entropy increase elicited by psychedelic drugs. Sci Rep **13**(1), 6244 (2023) https://doi.org/10.1038/s41598-023-32649-7

Hirschfeld, T., Schmidt, T.T.: Dose–response relationships of psilocybin-induced subjective experiences in humans. Journal of Psychopharmacology **35**(4), 384–397 (2021) https://doi.org/10.1177/0269881121992676

John Ashburner, Gareth Barnes, Chun-Chuan Chen, Jean Daunizeau, Guillaume Flandin, Karl Friston, Amirhossein Jafarian, Stefan Kiebel, James Kilner, Vladimir Litvak, Rosalyn Moran, Will Penny, Adeel Razi, Klaas Stephan, Sungho Tak, Peter Zeidman: SPM12 Manual. 4, vol. 2464. Wellcome Trust Centre for Neuroimaging, London, UK (2020)

Kaelen, M., Giribaldi, B., Raine, J., Evans, L., Timmerman, C., Rodriguez, N., Roseman, L., Feilding, A., Nutt, D., Carhart-Harris, R.: The hidden therapist: Evidence for a central role of music in psychedelic therapy. Psychopharmacology **235**(2), 505–519 (2018) https://doi.org/10.1007/s00213-017-4820-5

Khajehnejad, M., Habibollahi, F., Khajehnejad, A., Kagan, B.J., Razi, A.: TAVRNN: Temporal Attention-enhanced Variational Graph RNN Captures Neural Dynamics and Behavior. arXiv (2024). https://doi.org/10.48550/arXiv.2410.00665

Kundu, P., Inati, S.J., Evans, J.W., Luh, W.-M., Bandettini, P.A.: Differentiating BOLD and non-BOLD signals in fMRI time series using multi-echo EPI. NeuroImage **60**(3), 1759–1770 (2012) https://doi.org/10.1016/j.neuroimage.2011.12.028

Kwan, A.C., Olson, D.E., Preller, K.H., Roth, B.L.: The neural basis of psychedelic action. Nat Neurosci **25**(11), 1407–1419 (2022) https://doi.org/10.1038/s41593-022-01177-4

Kettner, H., Rosas, F.E., Timmermann, C., Kärtner, L., Carhart-Harris, R.L., Roseman, L.: Psychedelic Communitas: Intersubjective Experience During Psychedelic Group Sessions Predicts Enduring Changes in Psychological Wellbeing and Social Connectedness. Front Pharmacol **12**, 623985 (2021) https://doi.org/10.3389/fphar.2021.623985

Kometer, M., Schmidt, A., Jäncke, L., Vollenweider, F.X.: Activation of Serotonin 2A Receptors Underlies the Psilocybin-Induced Effects on α Oscillations, N170 Visual-Evoked Potentials, and Visual Hallucinations. J. Neurosci. **33**(25), 10544–10551 (2013) https://doi.org/10.1523/JNEUROSCI.3007-12.2013 . Chap. Articles

Lyons, T., Carhart-Harris, R.L.: Increased nature relatedness and decreased authoritarian political views after psilocybin for treatment-resistant depression. Journal of Psychopharmacology **32**(7), 811–819 (2018) https://doi.org/10.1177/0269881117748902

Ly, C., Greb, A.C., Cameron, L.P., Wong, J.M., Barragan, E.V., Wilson, P.C., Burbach, K.F., Soltanzadeh Zarandi, S., Sood, A., Paddy, M.R., Duim, W.C., Dennis, M.Y., McAllister, A.K., Ori-McKenney, K.M., Gray, J.A., Olson, D.E.: Psychedelics Promote Structural and Functional Neural Plasticity. Cell Reports **23**(11), 3170–3182 (2018) https://doi.org/10.1016/j.celrep.2018.05.022

Lempel, A., Ziv, J.: On the Complexity of Finite Sequences. IEEE Transactions on Information Theory **22**(1), 75–81 (1976) https://doi.org/10.1109/TIT.1976.1055501

Murphy, K., Birn, R.M., Handwerker, D.A., Jones, T.B., Bandettini, P.A.: The impact of global signal regression on resting state correlations: Are anti-correlated networks introduced? NeuroImage **44**(3), 893–905 (2009) https://doi.org/10.1016/j.neuroimage.2008.09.036

Ma, W.J., Beck, J.M., Latham, P.E., Pouget, A.: Bayesian inference with probabilistic population codes. Nat Neurosci **9**(11), 1432–8 (2006) https://doi.org/10.1038/nn1790

Margulies, D.S., Ghosh, S.S., Goulas, A., Falkiewicz, M., Huntenburg, J.M., Langs, G., Bezgin, G., Eickhoff, S.B., Castellanos, F.X., Petrides, M., Jefferies, E., Smallwood, J.: Situating the default-mode network along a principal gradient of macroscale cortical organization. Proceedings of the National Academy of Sciences **113**(44), 12574–12579 (2016) https://doi.org/10.1073/pnas.1608282113

Michaiel, A.M., Parker, P.R.L., Niell, C.M.: A Hallucinogenic Serotonin-2A Receptor Agonist Reduces Visual Response Gain and Alters Temporal Dynamics in Mouse V1. Cell reports **26**(13), 3475–34834 (2019) https://doi.org/10.1016/j.celrep.2019.02.104

Mediano, P.A.M., Rosas, F.E., Timmermann, C., Roseman, L., Nutt, D.J., Feilding, A., Kaelen, M., Kringelbach, M.L., Barrett, A.B., Seth, A.K., Muthukumaraswamy, S., Bor, D., Carhart-Harris, R.L.: Effects of External Stimulation on Psychedelic State Neurodynamics. ACS Chem. Neurosci. **15**(3), 462–471 (2024) https://doi.org/10.1021/acschemneuro.3c00289

Novelli, L., Friston, K., Razi, A.: Spectral dynamic causal modeling: A didactic introduction and its relationship with functional connectivity. Network Neuroscience **8**(1), 178–202 (2024) https://doi.org/10.1162/netn_a_00348

Nisbet, E.K., Zelenski, J.M.: The NR-6: A new brief measure of nature relatedness. Front Psychol **4**, 813 (2013) https://doi.org/10.3389/fpsyg.2013.00813

Oostenveld, R., Fries, P., Maris, E., Schoffelen, J.-M.: FieldTrip: Open Source Software for Advanced Analysis of MEG, EEG, and Invasive Electrophysiological Data. Computational Intelligence and Neuroscience **2011**(1), 156869 (2011) https://doi.org/10.1155/2011/156869

Oostenveld, R., Fries, P., Maris, E., Schoffelen, J.-M.: FieldTrip: Open Source Software for Advanced Analysis of MEG, EEG, and Invasive Electrophysiological Data. Computational Intelligence and Neuroscience **2011**(1), 156869 (2011) https://doi.org/10.1155/2011/156869

Olson, D.E.: The Subjective Effects of Psychedelics May Not Be Necessary for Their Enduring Therapeutic Effects. ACS Pharmacology & Translational Science (2020) https://doi.org/10.1021/acsptsci.0c00192

Palhano-Fontes, F., Andrade, K.C., Tofoli, L.F., Santos, A.C., Crippa, J.A., Hallak, J.E., Ribeiro, S., de Araujo, D.B.: The psychedelic state induced by ayahuasca modulates the activity and connectivity of the default mode network. Plos One **10**(2), 0118143 (2015) https://doi.org/10.1371/journal.pone.0118143

Preller, K.H., Burt, J.B., Ji, J.L., Schleifer, C.H., Adkinson, B.D., Stämpfli, P., Seifritz, E., Repovs, G., Krystal, J.H., Murray, J.D., Vollenweider, F.X., Anticevic, A.: Changes in global and thalamic brain connectivity in LSD-induced altered states of consciousness are attributable to the 5-HT2A receptor. eLife **7**, 35082 (2018) https://doi.org/10.7554/eLife.35082

Preller, K.H., Duerler, P., Burt, J.B., Ji, J.L., Adkinson, B., Stämpfli, P., Seifritz, E., Repovš, G., Krystal, J.H., Murray, J.D., Anticevic, A., Vollenweider, F.X.: Psilocybin Induces Time-Dependent Changes in Global Functional Connectivity. Biological Psychiatry **88**(2), 197–207 (2020) https://doi.org/10.1016/j.biopsych.2019.12.027

Parkes, L., Fulcher, B., Yücel, M., Fornito, A.: An evaluation of the efficacy, reliability, and sensitivity of motion correction strategies for resting-state functional MRI. NeuroImage **171**, 415–436 (2018) https://doi.org/10.1016/j.neuroimage.2017.12.073

Perl, Y.S., Geli, S., Pérez-Ordoyo, E., Zonca, L., Idesis, S., Vohryzek, J., Jirsa, V.K., Kringelbach, M.L., Tagliazucchi, E., Deco, G.: Modelling low-dimensional interacting brain networks reveals organising principle in human cognition. Network Neuroscience, 1–21 (2025) https://doi.org/10.1162/netn_a_00434

Pillai, A.S., Jirsa, V.K.: Symmetry Breaking in Space-Time Hierarchies Shapes Brain Dynamics and Behavior. Neuron **94**(5), 1010–1026 (2017) https://doi.org/10.1016/j.neuron.2017.05.013

Power, J.D., Mitra, A., Laumann, T.O., Snyder, A.Z., Schlaggar, B.L., Petersen, S.E.: Methods to detect, characterize, and remove motion artifact in resting state fMRI. NeuroImage **84**, 320–341 (2014) https://doi.org/10.1016/j.neuroimage.2013.08.048

Pokorny, T., Preller, K.H., Kometer, M., Dziobek, I., Vollenweider, F.X.: Effect of Psilocybin on Empathy and Moral Decision-Making. International Journal of Neuropsychopharmacology **20**(9), 747–757 (2017) https://doi.org/10.1093/ijnp/pyx047

Preller, K.H., Razi, A., Zeidman, P., Stämpfli, P., Friston, K.J., Vollenweider, F.X.: Effective connectivity changes in LSD-induced altered states of consciousness in humans. Proceedings of the National Academy of Sciences of the United States of America **116**(7), 2743–2748 (2019) https://doi.org/10.1073/pnas.1815129116

Preller, K.H., Vollenweider, F.X.: Phenomenology, Structure, and Dynamic of Psychedelic States. Curr Top Behav Neurosci **36**, 221–256 (2018) https://doi.org/10.1007/7854_2016_459

Ross, S., Bossis, A., Guss, J., Agin-Liebes, G., Malone, T., Cohen, B., Mennenga, S.E., Belser, A., Kalliontzi, K., Babb, J., Su, Z., Corby, P., Schmidt, B.L.: Rapid and sustained symptom reduction following psilocybin treatment for anxiety and depression in patients with life-threatening cancer: A randomized controlled trial. Journal of Psychopharmacology **30**(12), 1165–1180 (2016) https://doi.org/10.1177/0269881116675512

Reker, G.T.: Manual of the Life Attitude Profile–Revised (LAP-R). Student Psychologists Press, Peterborough, Ontario (1992)

Razi, A., Friston, K.J.: The Connected Brain: Causality, models, and intrinsic dynamics. IEEE Signal Processing Magazine **33**(3), 14–35 (2016) https://doi.org/10.1109/MSP.2015.2482121

Razi, A., Kahan, J., Rees, G., Friston, K.J.: Construct validation of a DCM for resting state fMRI. NeuroImage **106**, 1–14 (2015) https://doi.org/10.1016/j.neuroimage.2014.11.027

Raichle, M.E., MacLeod, A.M., Snyder, A.Z., Powers, W.J., Gusnard, D.A., Shulman, G.L.: A default mode of brain function. Proc Natl Acad Sci U S A **98**(2), 676–82 (2001) https://doi.org/10.1073/pnas.98.2.676

Roseman, L., Nutt, D.J., Carhart-Harris, R.L.: Quality of Acute Psychedelic Experience Predicts Therapeutic Efficacy of Psilocybin for Treatment-Resistant Depression. Frontiers in Pharmacology **8**, 974 (2018) https://doi.org/10.3389/fphar.2017.00974

Rubinov, M., Sporns, O.: Complex network measures of brain connectivity: Uses and interpretations. NeuroImage **52**(3), 1059–1069 (2010) https://doi.org/10.1016/j.neuroimage.2009.10.003

Rubinov, M., Sporns, O.: Weight-conserving characterization of complex functional brain networks. NeuroImage **56**(4), 2068–2079 (2011) https://doi.org/10.1016/j.neuroimage.2011.03.069

Reinwald, J.R., Schmitz, C.N., Skorodumov, I., Kuchar, M., Weber-Fahr, W., Spanagel, R., Meinhardt, M.W.: Psilocybin-induced default mode network hypoconnectivity is blunted in alcohol-dependent rats. Translational psychiatry **13**(1), 392 (2023) https://doi.org/10.1038/s41398-023-02690-1

Smallwood, J., Bernhardt, B.C., Leech, R., Bzdok, D., Jefferies, E., Margulies, D.S.: The default mode network in cognition: A topographical perspective. Nat Rev Neurosci **22**(8), 503–513 (2021) https://doi.org/10.1038/s41583-021-00474-4

Schartner, M.M., Carhart-Harris, R.L., Barrett, A.B., Seth, A.K., Muthukumaraswamy, S.D.: Increased spontaneous MEG signal diversity for psychoactive doses of ketamine, LSD and psilocybin. Sci Rep **7**(1), 46421 (2017) https://doi.org/10.1038/srep46421

Sachs, M.E., Ellis, R.J., Schlaug, G., Loui, P.: Brain connectivity reflects human aesthetic responses to music. Social cognitive and affective neuroscience **11**(6), 884–91 (2016) https://doi.org/10.1093/scan/nsw009

Somers, B., Francart, T., Bertrand, A.: A generic EEG artifact removal algorithm based on the multi-channel Wiener filter. J. Neural Eng. **15**(3), 036007 (2018) https://doi.org/10.1088/1741-2552/aaac92

Studerus, E., Gamma, A., Vollenweider, F.X.: Psychometric evaluation of the altered states of consciousness rating scale (OAV). Plos One **5**(8), 12412–12412 (2010) https://doi.org/10.1371/journal.pone.0012412

Schmidt, M., Hoffrichter, A., Davoudi, M., Horschitz, S., Lau, T., Meinhardt, M., Spanagel, R., Ladewig, J., Köhr, G., Koch, P.: Psilocin Fosters Neuroplasticity in iPSC-derived Human Cortical Neurons, (2024)

Schaefer, A., Kong, R., Gordon, E.M., Laumann, T.O., Zuo, X.-N., Holmes, A.J., Eickhoff, S.B., Yeo, B.T.T.: Local-Global Parcellation of the Human Cerebral Cortex from Intrinsic Functional Connectivity MRI. Cerebral Cortex **28**(9), 3095–3114 (2018) https://doi.org/10.1093/cercor/bhx179

Shao, L.X., Liao, C., Gregg, I., Davoudian, P.A., Savalia, N.K., Delagarza, K., Kwan, A.C.: Psilocybin induces rapid and persistent growth of dendritic spines in frontal cortex in vivo. Neuron **109**(16), 2535–25444 (2021) https://doi.org/10.1016/j.neuron.2021.06.008

Schneider, S., Lee, J.H., Mathis, M.W.: Learnable latent embeddings for joint behavioural and neural analysis. Nature **617**(7960), 360–368 (2023) https://doi.org/10.1038/s41586-023-06031-6

Smith, S.M., Nichols, T.E.: Threshold-free cluster enhancement: Addressing problems of smoothing, threshold dependence and localisation in cluster inference. NeuroImage **44**(1), 83–98 (2009) https://doi.org/10.1016/j.neuroimage.2008.03.061

Silvia, P.J., Nusbaum, E.C.: On personality and piloerection: Individual differences in aesthetic chills and other unusual aesthetic experiences. Psychology of Aesthetics, Creativity, and the Arts **5**, 208–214 (2011)

Stoliker, D., Novelli, L., Vollenweider, F.X., Egan, G.F., Preller, K.H., Razi, A.: Neural Mechanisms of Resting-State Networks and the Amygdala Underlying the Cognitive and Emotional Effects of Psilocybin. Biological Psychiatry **96**(1), 57–66 (2024) https://doi.org/10.1016/j.biopsych.2024.01.002

Stoliker, D., Novelli, L., Vollenweider, F.X., Egan, G.F., Preller, K.H., Razi, A.: Effective Connectivity of Functionally Anticorrelated Networks Under Lysergic Acid Diethylamide. Biological Psychiatry **93**, 224–232 (2023) https://doi.org/10.1016/j.biopsych.2022.07.013

Stoliker, D., Preller, K.H., Novelli, L., Anticevic, A., Egan, G.F., Vollenweider, F.X., Razi, A.: Neural mechanisms of psychedelic visual imagery. Mol Psychiatry, 1–8 (2024) https://doi.org/10.1038/s41380-024-02632-3

Siegel, J.S., Subramanian, S., Perry, D., Kay, B.P., Gordon, E.M., Laumann, T.O., Reneau, T.R., Metcalf, N.V., Chacko, R.V., Gratton, C., Horan, C., Krimmel, S.R., Shimony, J.S., Schweiger, J.A., Wong, D.F., Bender, D.A., Scheidter, K.M., Whiting, F.I., Padawer-Curry, J.A., Shinohara, R.T., Chen, Y., Moser, J., Yacoub, E., Nelson, S.M., Vizioli, L., Fair, D.A., Lenze, E.J., Carhart-Harris, R., Raison, C.L., Raichle, M.E., Snyder, A.Z., Nicol, G.E., Dosenbach, N.U.F.: Psilocybin desynchronizes the human brain. Nature **632**(8023), 131–138 (2024) https://doi.org/10.1038/s41586-024-07624-5

Stamatopoulou, D.: Integrating the philosophy and psychology of aesthetic experience: development of the aesthetic experience scale. Psychological Reports **95**(2), 673–695 (2004) https://doi.org/10.2466/pr0.95.2.673-695

Sporns, O., Tononi, G., Kötter, R.: The human connectome: A structural description of the human brain. PLoS Comput Biol **1**(4), 42 (2005) https://doi.org/10.1371/journal.pcbi.0010042

Swanson, L.R.: Unifying Theories of Psychedelic Drug

Effects. Frontiers in Pharmacology **9**(172) (2018) https://doi.org/10.3389/fphar.2018.00172

Tagliazucchi, E., Carhart-Harris, R., Leech, R., Nutt, D., Chialvo, D.R.: Enhanced repertoire of brain dynamical states during the psychedelic experience. Human Brain Mapping **35**(11), 5442–5456 (2014) https://doi.org/10.1002/hbm.22562

Tian, Y., Margulies, D.S., Breakspear, M., Zalesky, A.: Topographic organization of the human subcortex unveiled with functional connectivity gradients. Nature Neuroscience **23**(11), 1421–1432 (2020) https://doi.org/10.1038/s41593-020-00711-6

Toscani, M., Marzi, T., Righi, S., Viggiano, M.P., Baldassi, S.: Alpha waves: A neural signature of visual suppression. Experimental Brain Research **207**(3), 213–219 (2010) https://doi.org/10.1007/s00221-010-2444-7

Timmermann, C., Roseman, L., Haridas, S., Rosas, F.E., Luan, L., Kettner, H., Martell, J., Erritzoe, D., Tagliazucchi, E., Pallavicini, C., Girn, M., Alamia, A., Leech, R., Nutt, D.J., Carhart-Harris, R.L.: Human brain effects of DMT assessed via EEG-fMRI. Proc. Natl. Acad. Sci. U.S.A. **120**(13), 2218949120 (2023) https://doi.org/10.1073/pnas.2218949120

Tagliazucchi, E., Roseman, L., Kaelen, M., Orban, C., Muthukumaraswamy, S.D., Murphy, K., Laufs, H., Leech, R., McGonigle, J., Crossley, N., Bullmore, E., Williams, T., Bolstridge, M., Feilding, A., Nutt, D.J., Carhart-Harris, R.: Increased Global Functional Connectivity Correlates with LSD-Induced Ego Dissolution. Current Biology **26**(8), 1043–1050 (2016) https://doi.org/10.1016/j.cub.2016.02.010

Vollenweider, F.X., Kometer, M.: The neurobiology of psychedelic drugs: Implications for the treatment of mood disorders. Nature Reviews Neuroscience **11**(9), 642–651 (2010) https://doi.org/10.1038/nrn2884

Vaidya, V.A., Marek, G.J., Aghajanian, G.K., Duman, R.S.: 5-HT $_{2A}$ Receptor-Mediated Regulation of Brain-Derived Neurotrophic Factor mRNA in the Hippocampus and the Neocortex. The Journal of Neuroscience **17**(8), 2785–2795 (1997) https://doi.org/10.1523/JNEUROSCI.17-08-02785.1997

Viol, A., Palhano-Fontes, F., Onias, H., de Araujo, D.B., Hövel, P., Viswanathan, G.M.: Characterizing Complex Networks Using Entropy-Degree Diagrams: Unveiling Changes in Functional Brain Connectivity Induced by Ayahuasca. Entropy (Basel) **21**(2) (2019) https://doi.org/10.3390/e21020128

Watts, R., Day, C., Krzanowski, J., Nutt, D., Carhart-Harris, R.: Patients' Accounts of Increased "Connectedness" and "Acceptance" After Psilocybin for Treatment-Resistant Depression. Journal of Humanistic Psychology **57**(5), 520–564 (2017) https://doi.org/10.1177/0022167817709585

Yaden, D.B., Griffiths, R.R.: The Subjective Effects of Psychedelics Are Necessary for Their Enduring Therapeutic Effects. ACS Pharmacology & Translational Science (2020) https://doi.org/10.1021/acsptsci.0c00194

Zeidman, P., Jafarian, A., Seghier, M.L., Litvak, V., Cagnan, H., Price, C.J., Friston, K.J.: A guide to group effective connectivity analysis, part 2: Second level analysis with PEB. NeuroImage **200**, 12–25 (2019) https://doi.org/10.1016/j.neuroimage.2019.06.032

Extended Data

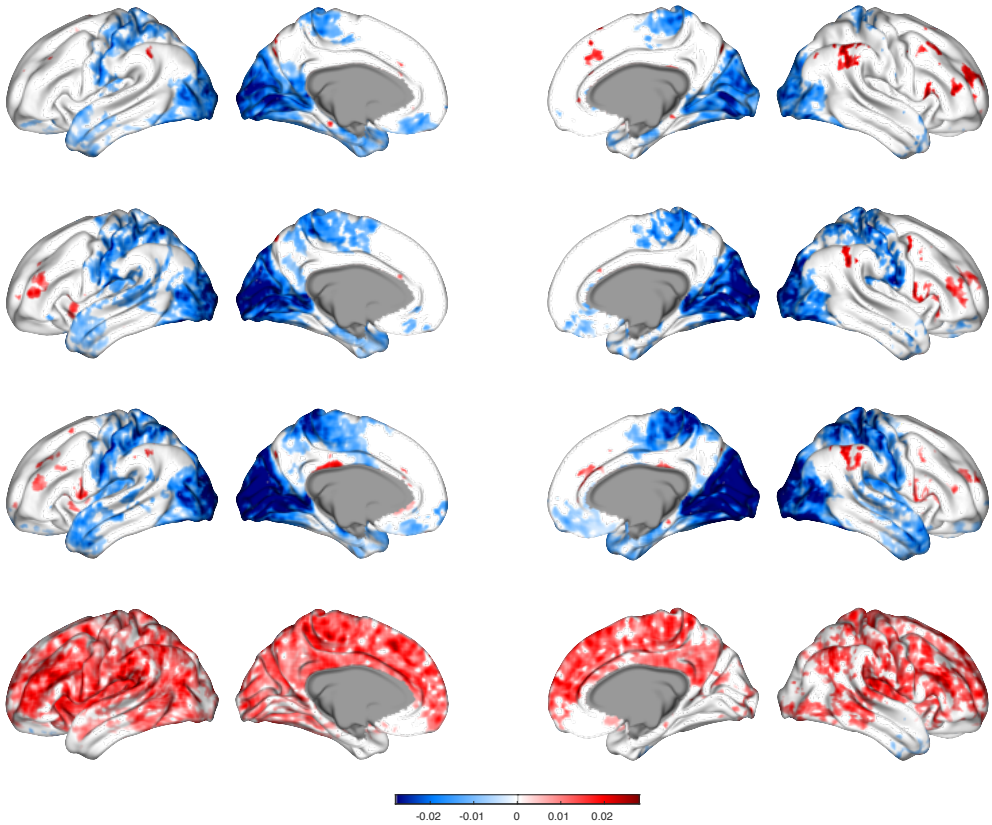

Fig. Extended Data 1 Significant GFC clusters at $p < 0.05$ after threshold-free cluster enhancement (TFCE).

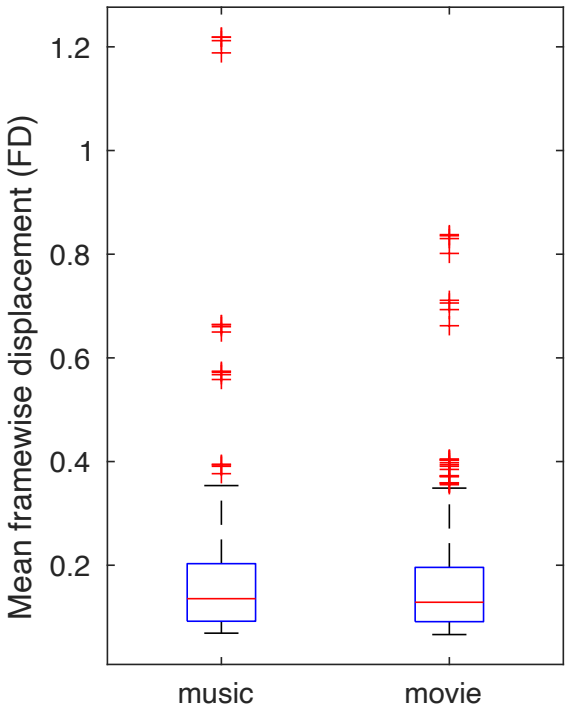

Fig. Extended Data 2 Head motion comparison between music and movie conditions, quantified via the mean frame-wise displacement. No statistical significant differences were observed.

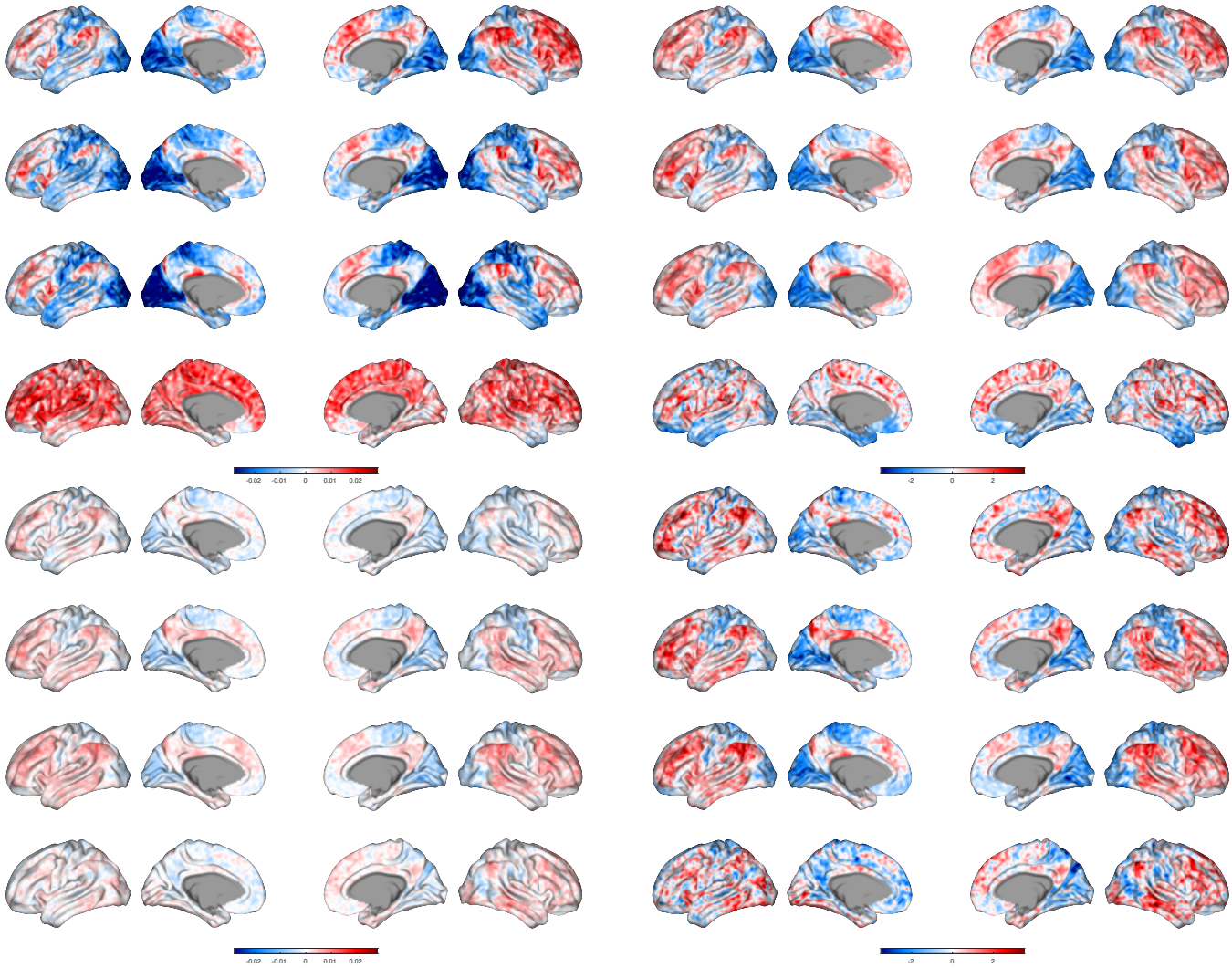

Fig. Extended Data 3 a) GFC b) z-score c) GSR d) GSR and z-score

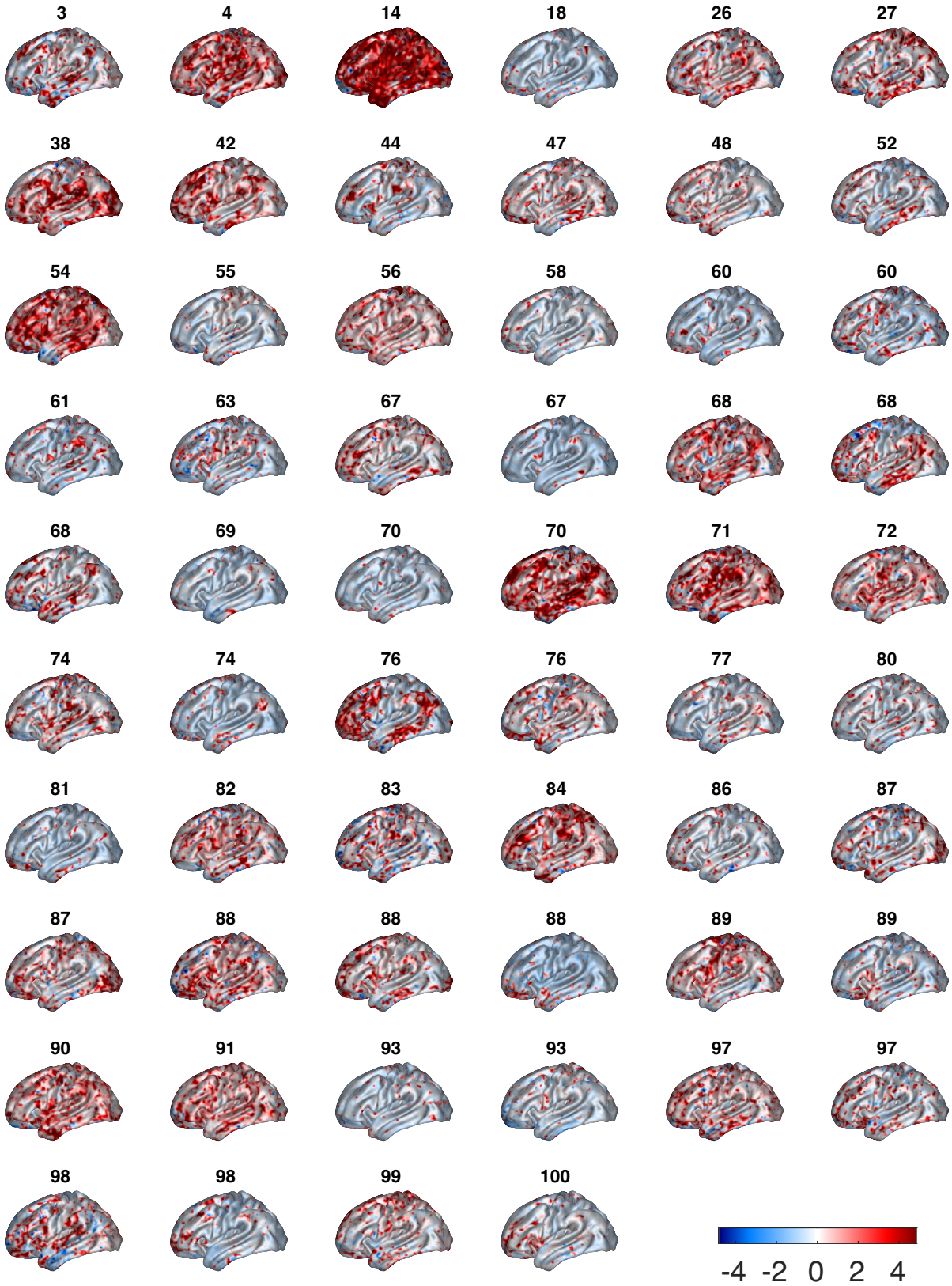

Fig. Extended Data 4 Despite the statistically significant group differences, GFC is highly variable across subjects, even when the subjective effects measured via the Mystical Experience Questionnaire (MEQ30) are similar. Here, the subjects are sorted by MEQ30 values and the individual GFC percentage difference maps (psilocybin minus baseline, divided by baseline) are shown for the resting-state condition.

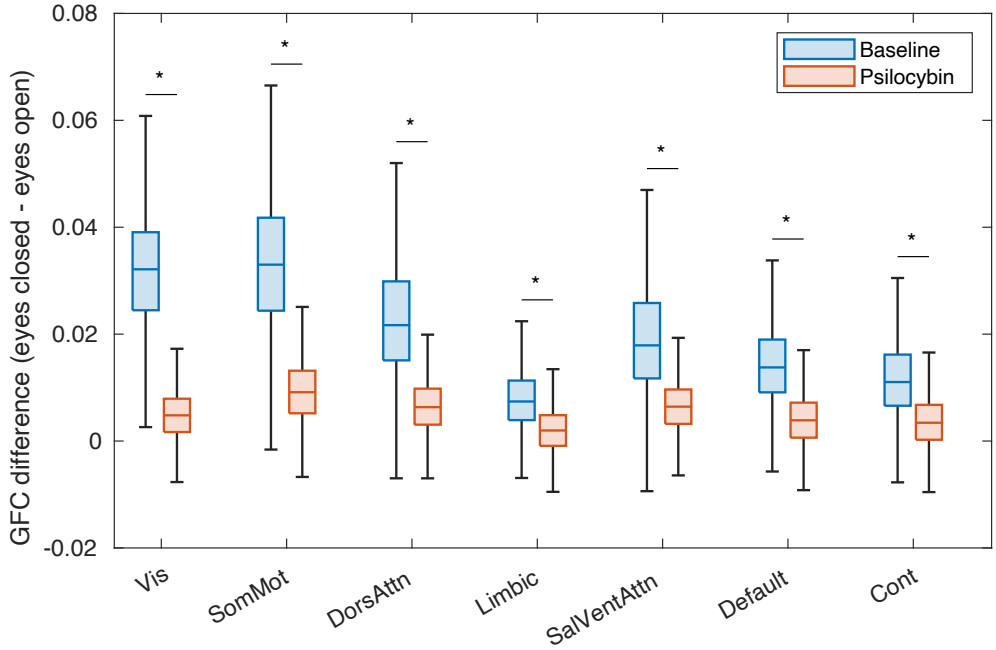

Fig. Extended Data 5 The GFC difference between eyes-closed and eyes-open conditions decreased after psilocybin administration. The largest effect was observed in the visual network (-85%, with a robust Cohen's d effect size of -3.23), but the reduction was larger than -66% and highly statistically significant in all Schaefer networks (Mann-Whitney U-test right-tailed p-values $p < 10^{-307}$).

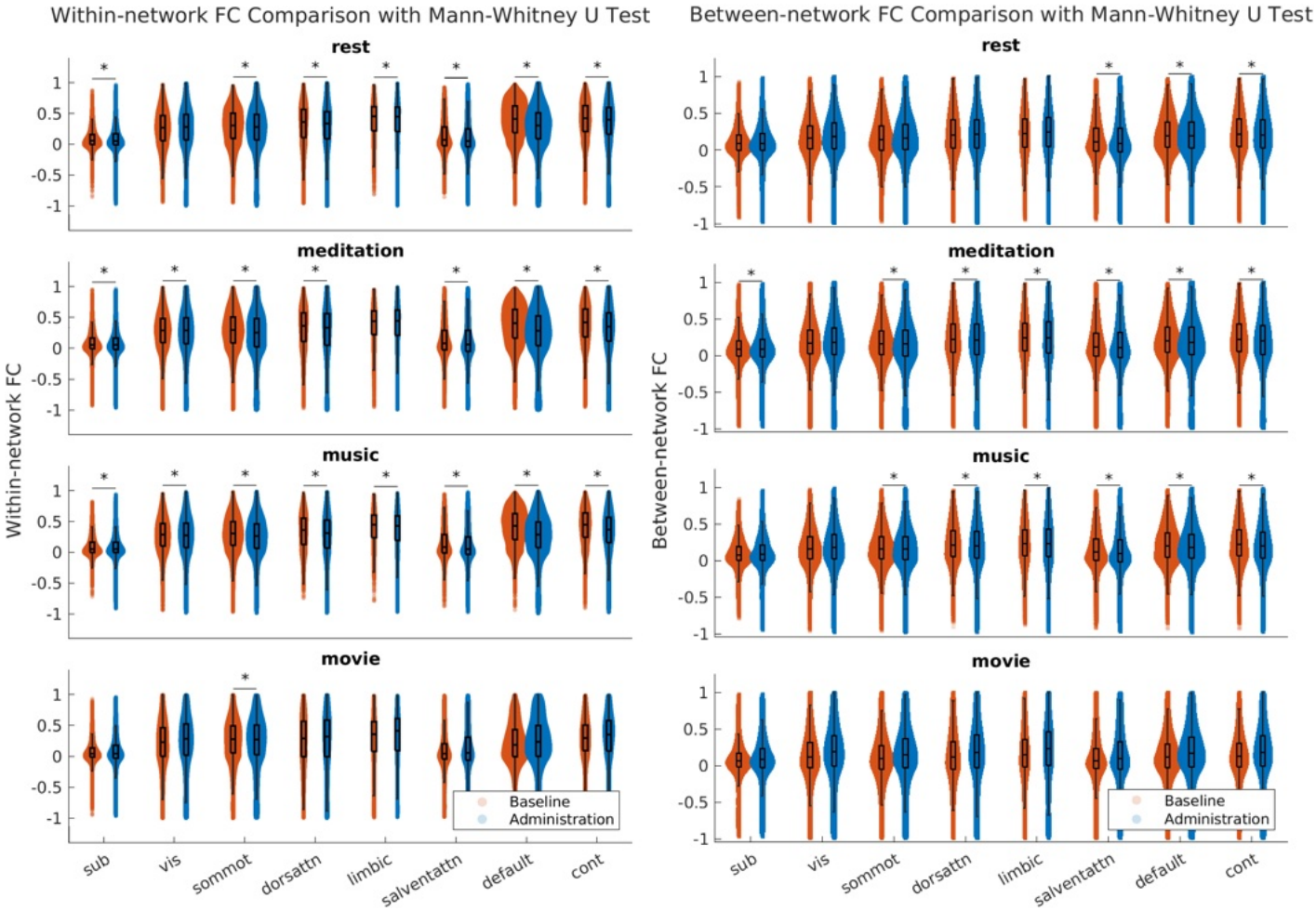

Fig. Extended Data 6 a) Psilocybin reduces functional connectivity within most networks during the eyes-closed conditions: resting-state, meditation, and music. The decrease in functional connectivity is strongest in the default-mode network (DMN). Conversely, during the movie, the within-network functional connectivity only decreases in the somato-motor network but increases in most of the other networks, particularly in the DMN. b) Psilocybin reduces functional connectivity between most networks and the rest of the brain during the eyes-closed conditions. Each swarm chart and box plot indicates the average functional connectivity between one network and the rest of the brain. The strongest decrease in functional connectivity is between the default-mode network (DMN) and the rest of the brain. Conversely, during the movie, the functional connectivity increases between most networks, particularly the DMN. Each star symbol indicates a significant decrease based on the Mann-Whitney U-test ($\alpha = 0.00625$ to correct for multiple comparisons across eight resting-state networks).

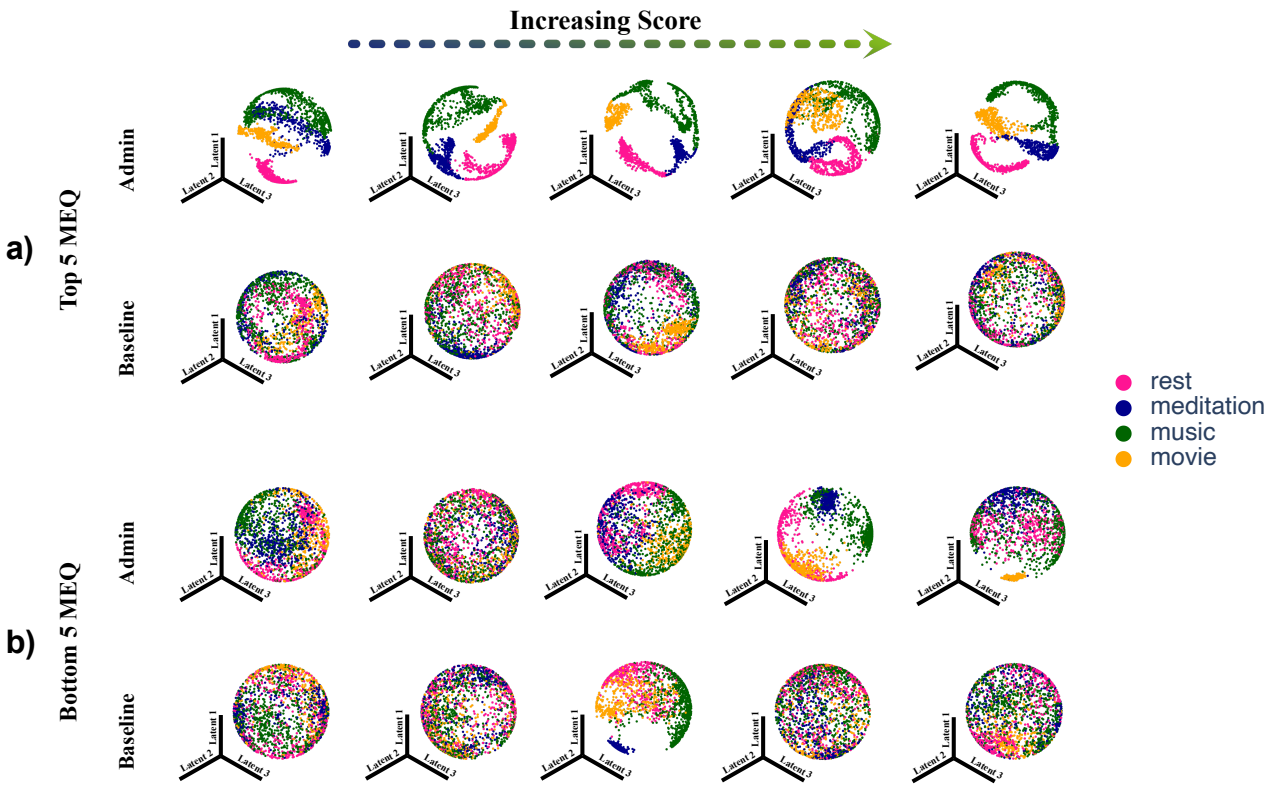

Fig. Extended Data 7 Trajectories derived using the CEBRA method, mapped into 3D space for participants with the a) top and b) bottom five MEQ scores for both baseline (no psilocybin) and psilocybin sessions. Pink, blue, green, and yellow segments represent rest, meditation, music, and movie conditions, respectively.

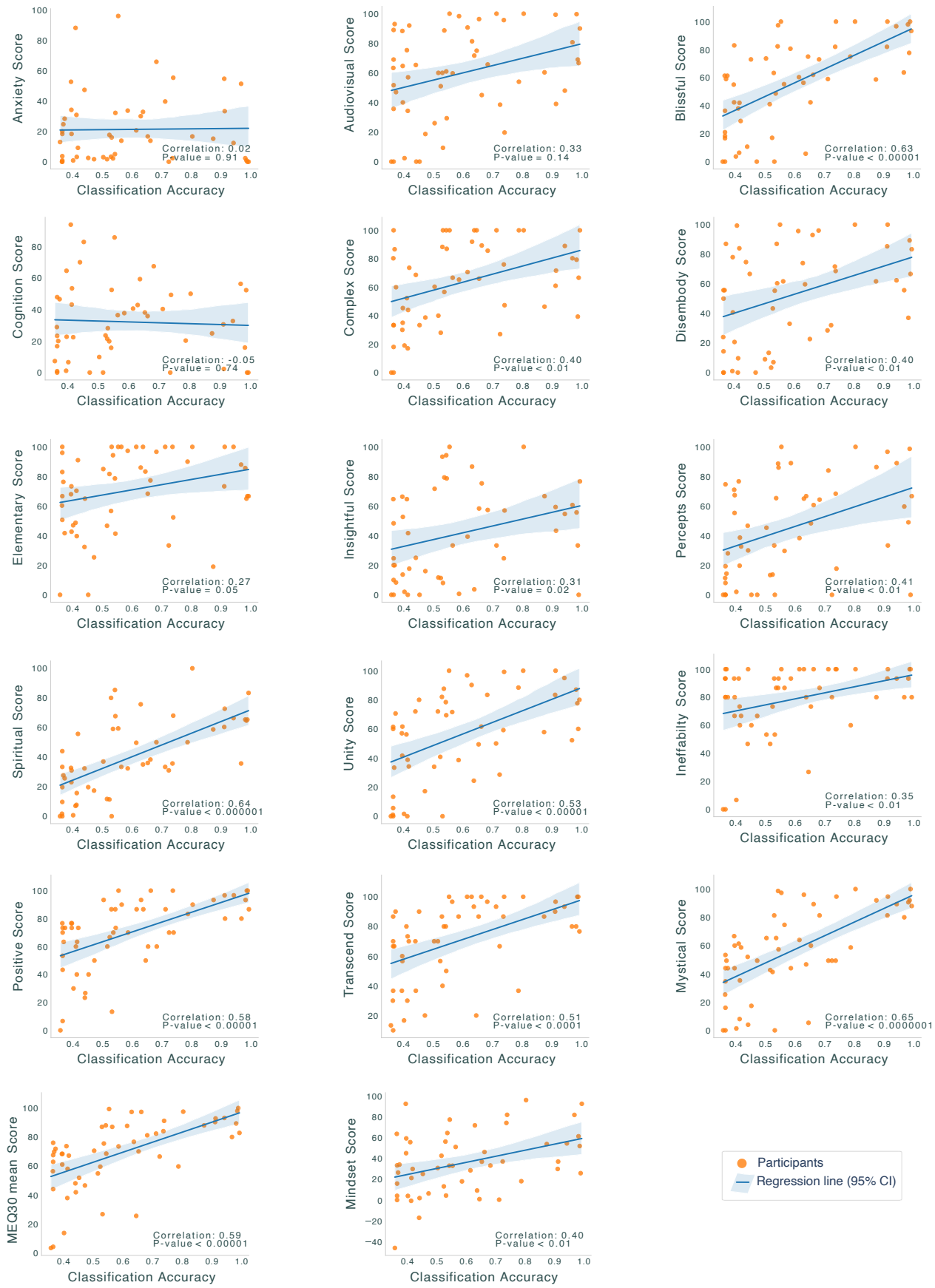

Fig. Extended Data 8 For each participant's CEBRA trajectory, a Support Vector Machine (SVM) was used to classify the correct condition label at each time point. The figure also presents the Pearson correlation between classification accuracy and participants' 11D ASC, Mindset, MEQ30, and MEQ30 mean scores, reporting the correlation coefficient and statistical significance level (p-value ≤ 0.05, uncorrected). The blue solid line represents the regression fit, with the shaded region indicating the 95% confidence interval.

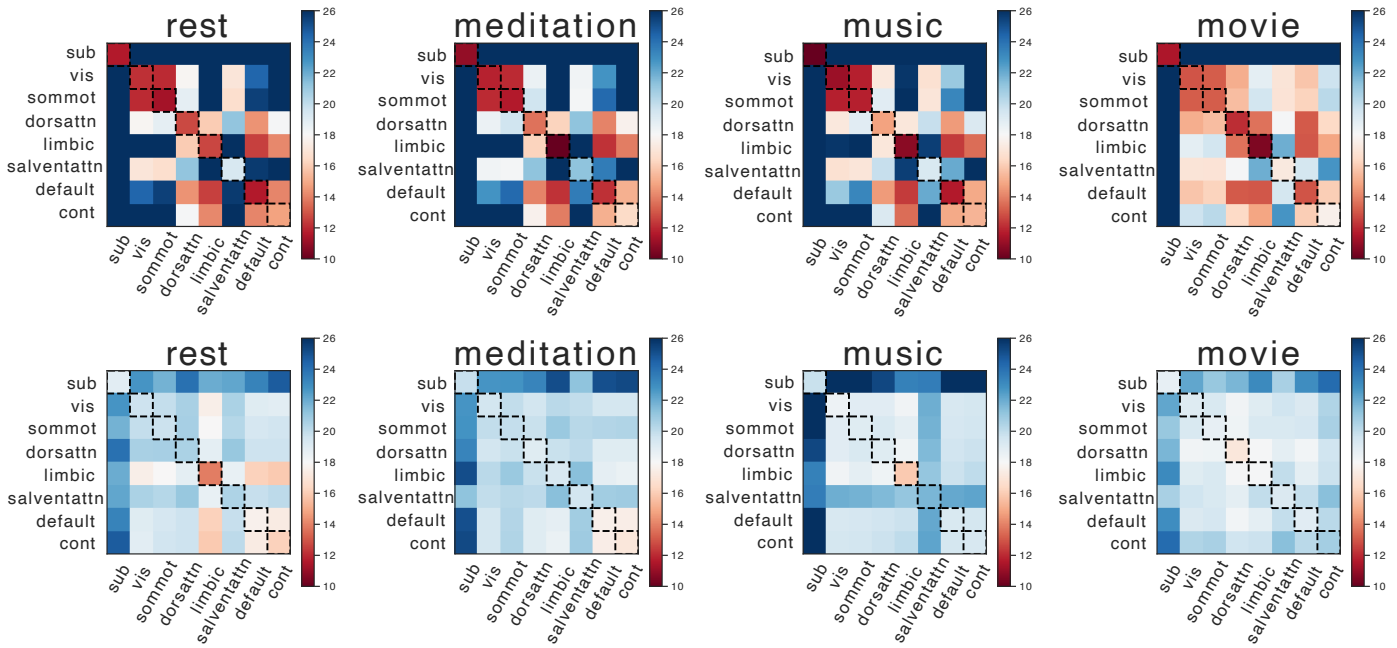

Fig. Extended Data 9 Heatmaps showing the average Euclidean distance between pairs of ROIs within each brain network in the TAVRNN embedding space across the four cognitive conditions: rest, meditation, music, and movie. The top row represents the heatmaps for participants with the top 5 MEQ scores, and the bottom row represents the heatmaps for participants with the lowest 5 MEQ scores. For all conditions, the diagonal of the top row exhibits higher values, indicating more densely clustered embeddings (ROIs positioned closer to each other) within the same network compared to the bottom row, which suggests a greater spread of ROIs in participants with lower MEQ scores.

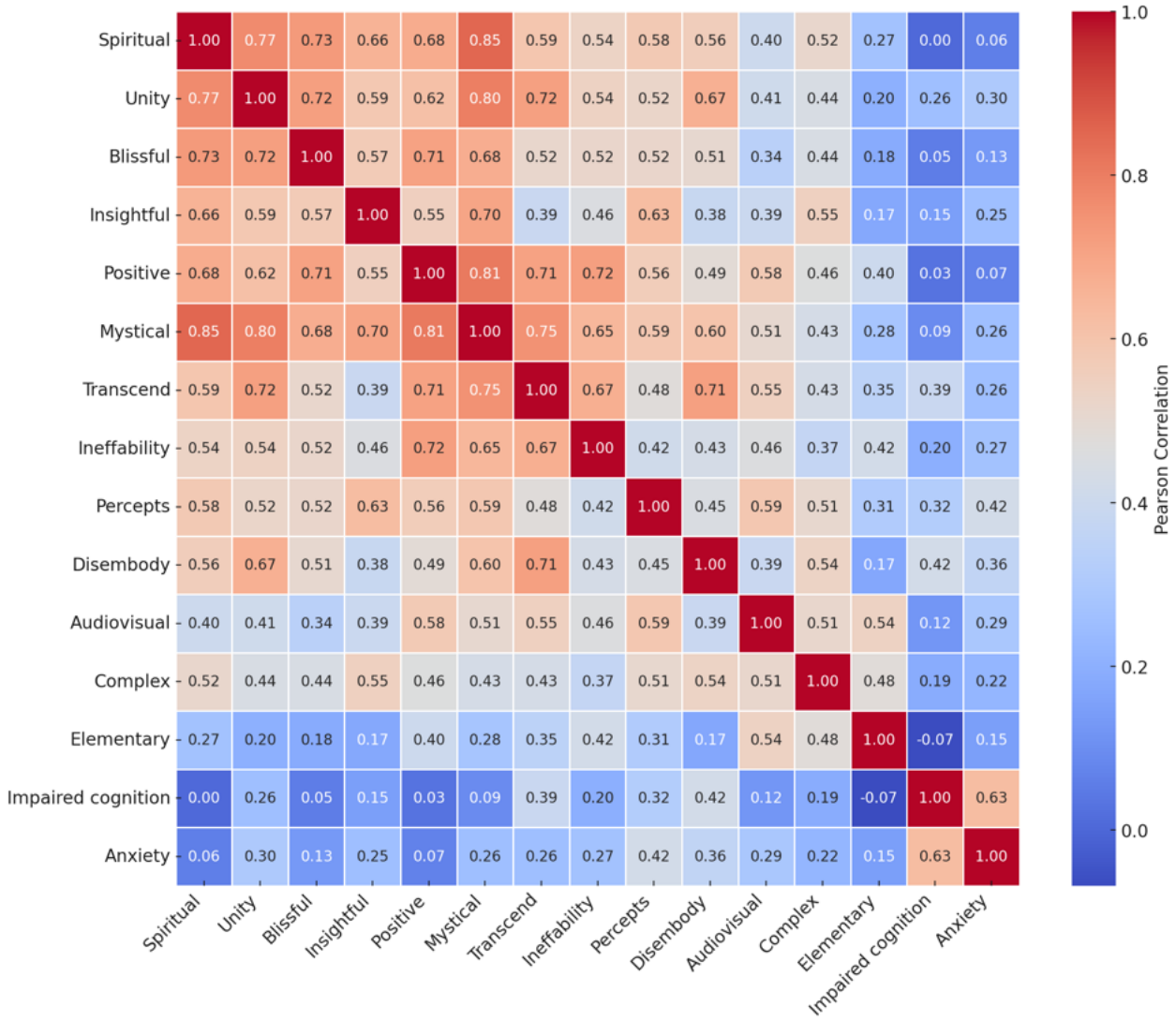

Fig. Extended Data 10 Matrix of correlation between MEQ and 11D ASC subscales, derived from our samples scores.

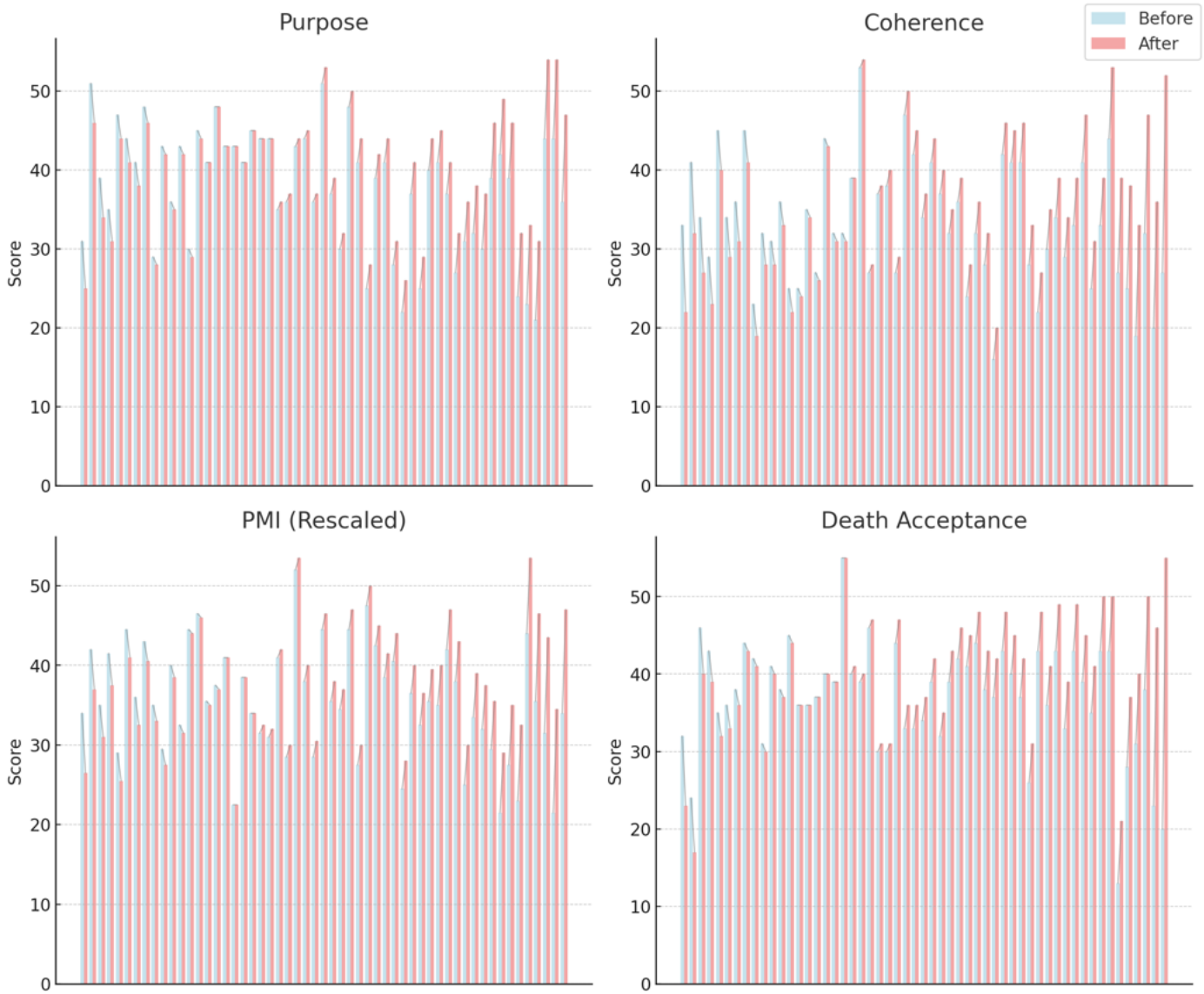

Fig. Extended Data 11 Individual Variability in Changes in Life Attitudes (LAP-R) dimensions Before and One Month After Psilocybin. Each panel displays individual participant changes for Purpose, Coherence, Personal Meaning Index (PMI) (Purpose + Coherence), and Death Acceptance. Participants are sorted by change magnitude, from largest decrease to largest increase. Each participant has two bars: blue (before psilocybin) and red (after psilocybin), with gray linking lines indicating the change for each individual. Personal Meaning was rescaled by dividing the score by 2. At the group level, paired t-tests revealed statistically significant improvements: Purpose: $t(54) = -3.87$, $p = 0.0003$, $d = 0.52$ (moderate effect). Coherence: $t(54) = -2.81$, $p = 0.0069$, $d = 0.38$ (small-to-moderate effect). Personal Meaning (Purpose + Coherence): $t(54) = -3.77$, $p = 0.0004$, $d = 0.51$ (moderate effect). Death Acceptance: $t(54) = -3.66$, $p = 0.0006$, $d = 0.49$ (moderate effect). These results indicate group-level increases in all four dimensions of interest post-psilocybin, while also highlighting substantial individual variability in response patterns. Some participants showed large increases, while others exhibited minimal or negative changes. The linking lines emphasize heterogeneity in individual responses, demonstrating that while the overall effect is positive, not all participants experience the same degree of change.

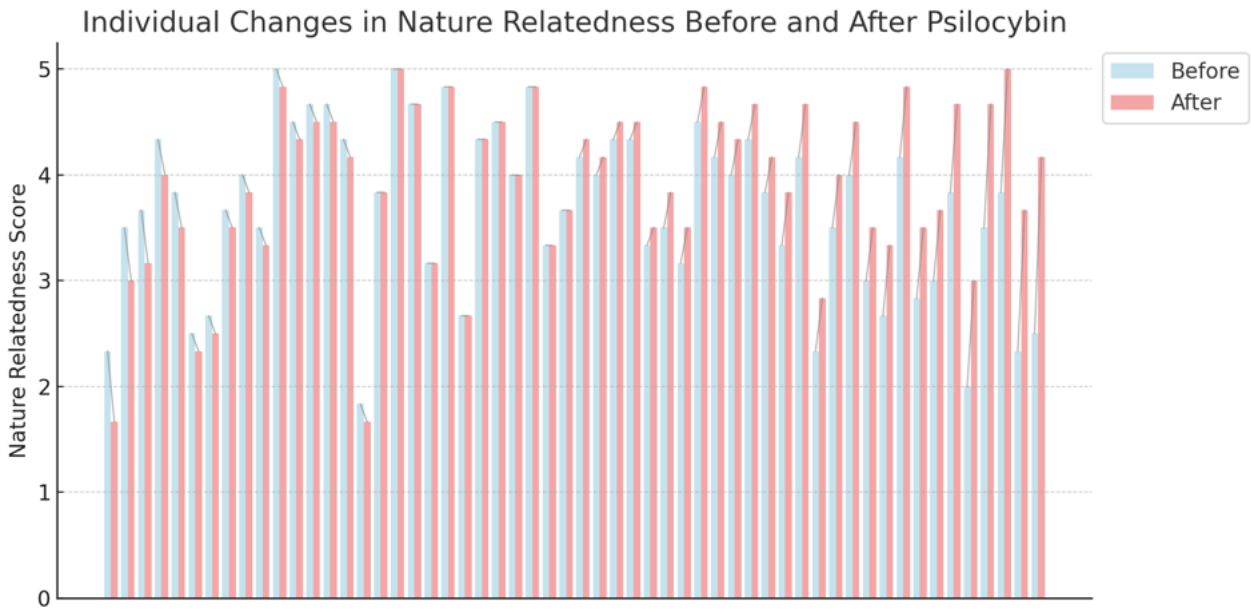

Fig. Extended Data 12 Individual Variability in Changes in Nature Relatedness Before and One Month After Psilocybin. Participants are sorted by change magnitude, from largest decrease to largest increase. Each participant has two bars: blue (before psilocybin) and red (after psilocybin), with gray linking lines indicating the change for each individual. At the group level, paired t-tests revealed statistically significant improvements t(55) = -3.37, p = 0.0014, d = 0.26 (moderate effect).

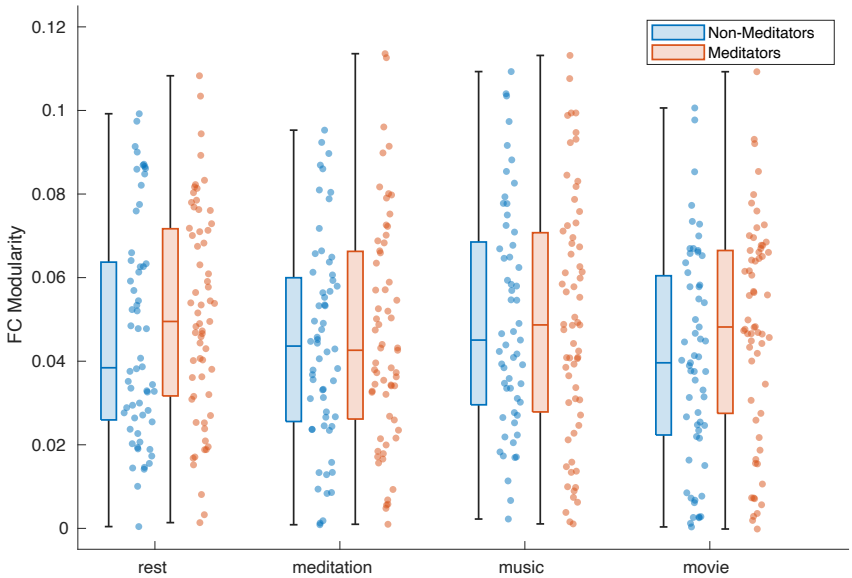

Fig. Extended Data 13 Meditation training didn't result in statistically significant changes in functional modularity.

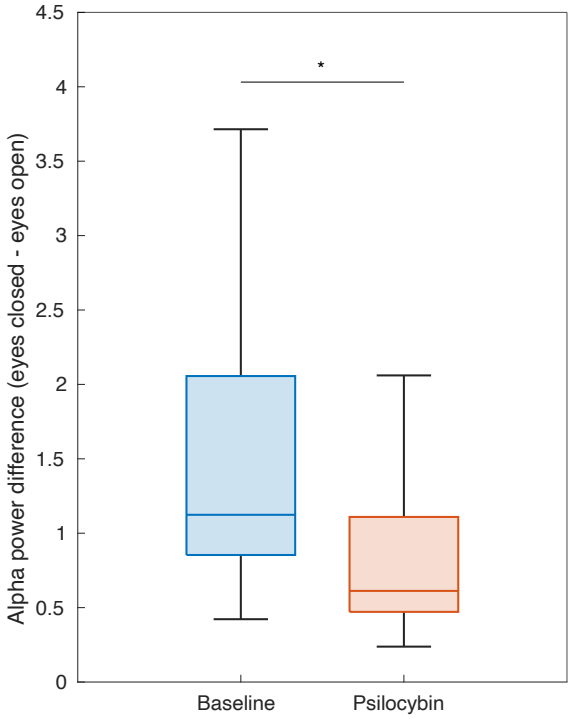

Fig. Extended Data 14 The alpha power difference between eyes-closed and eyes-open conditions decreased by 48% after psilocybin administration (robust Cohen's $d = -0.79$, Mann-Whitney U-test right-tailed p-value $< 10^{-19}$).